

AD 74 4806

INSTITUTE OF GAS TECHNOLOGY

DDC
RECEIVED
JUN 19 1972
B

NATIONAL TECHNICAL
INFORMATION SERVICE

3424 SOUTH STATE STREET

IIT CENTER

CHICAGO, ILLINOIS 60616

AFFILIATED WITH ILLINOIS INSTITUTE OF TECHNOLOGY

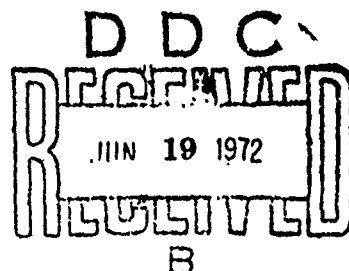
 **IGT**
EDUCATION • RESEARCH

INSTITUTE OF GAS TECHNOLOGY
IIT CENTER
CHICAGO, ILLINOIS 60616

LOW-COST ACID FUEL CELL STACKS

Final Report

June 1972



IGT PROJECT NO. 8902

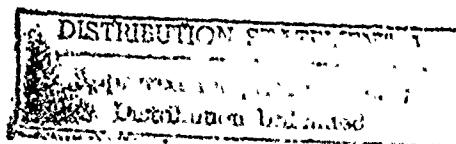
U.S. ARMY CONTRACT DAAK 02-67-C-0063

Prepared for

RESEARCH AND DEVELOPMENT PROCUREMENT OFFICE

U.S. ARMY MOBILITY EQUIPMENT RESEARCH
AND DEVELOPMENT CENTER

Ft. Belvoir, Virginia 22060



NOTICESDISCLAIMERS

The findings in this report are not to be construed as an official Department of the Army position, unless so designated by other authorized documents.

The citation of the trade names and the names of the manufacturers in this report is not to be construed as official Government endorsement or approval of the commercial products or services referenced herein.

DISPOSITION

Destroy this report when it is no longer needed. Do not return it to the originator.

DISTRIBUTION

This document is approved for public release; distribution unlimited.

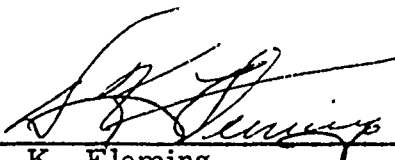
Preceding page blank

IGT Project No. 8902

U.S. ARMY CONTRACT DAAK 02-67-C-0063

The work effort for this project was conducted at the IGT Energy Conversion Research Laboratory.

Signed



D. K. Fleming
Supervisor
Low-Temperature Fuel Cell Research

Approved



R. B. Rosenberg
Director
Engineering Research

Preceding page blank

FOREWORD

This is the final report on a research program to redesign and to improve compact, low-temperature, acid electrolyte fuel cell stacks. These stacks, which utilize low-platinum loading electrodes, are operated on air and reformed CITE fuel or combat gasoline.

This report is prepared by the Institute of Gas Technology, in accordance with provisions in Contract No. DAAK 02-67-C-0063, for the U.S. Army Mobility Equipment Research and Development Center, Fort Belvoir, Virginia 22060.

TABLE OF CONTENTS

	<u>Page</u>
1. SUMMARY	1
2. OBJECTIVE	6
3. INTRODUCTION	7
3.1. History	7
3.1.1. Initial Work	7
3.1.2. Earlier Work Under This Contract	8
3.2. Present Program	9
3.3. Contract Modifications	10
3.4. Future Work	10
4. PREVIOUS DESIGN	11
4.1. History	13
4.2. Deficiencies of Previous Design	17
4.2.1. Materials of Construction	17
4.2.2. Design Problems	18
4.2.3. Manufacturing Techniques	20
5. NEW HARDWARE DESIGN	21
5.1. Design Philosophy	21
5.2. Bipolar Plates	22
5.2.1. Constructional Material	23
5.2.2. Bipolar Plate — Embossing Pattern	24
5.2.3. Bipolar Plate — Hydraulic Considerations	31
5.2.3.1. Pressure Drop Along the Cell Face	34
5.2.3.2. Pressure Drop Through Inlet Orifices	35
5.2.3.3. Other Pressure Drops	36
5.2.3.4. Physical Design of Bipolar Plate Hydraulic Components	37
5.3. Gas Compartment Frames	40
5.3.1. Earlier Design	40
5.3.2. Materials of Construction	40

TABLE OF CONTENTS, Cont.

	<u>Page</u>
5.3.3. Flow Distribution	42
5.3.4. Pressure Drops	43
5.4. Cell Gasketing	47
5.5. Electrodes	48
5.5.1. Cathodes	48
5.5.2. Anodes	49
5.5.3. Alternative Electrode Sources	49
5.6. Matrices	50
5.6.1. American Cyanamid Teflon Matrices	50
5.6.2. Union Carbide Tantalum Oxide Matrix	51
5.6.3. Pratt & Whitney Matrix	52
5.6.4. Matrices Used During Tests	52
5.7. Coolant Plates	52
5.7.1. Previous Design	53
5.7.2. Liquid Coolant Plates	54
5.7.2.1. Liquid Coolant Plates – Hydraulic Design	55
5.7.2.2. Liquid Coolant Plates – Mechanical Design	56
5.7.2.3. Liquid Coolant Plates – Corrosion Protection	57
5.7.2.4. Liquid Coolant Plates – Operational Difficulties	60
5.7.3. Air-Cooling Plates	63
5.7.3.1. Air-Coolant Plates – Hydraulic and Thermal Considerations	64
5.7.3.2. Mechanical Construction	65
5.8. End Plates	68
5.8.1. Previous Design	68
5.8.2. End Plate – Structural Design	69
5.8.3. End Plate – Construction	70
5.9. Assembly	74

TABLE OF CONTENTS, Cont.

	<u>Page</u>
6. TESTING AND OPERATION	78
6.1. Small-Cell Tests	78
6.2. Small-Stack Tests	79
6.3. Large-Module Tests	80
6.3.1. Liquid-Cooled Modules	80
6.3.2. Air-Cooled Modules	81
6.4. Stack Operation	81
6.4.1. Design Criteria	81
6.4.2. Design Compromises	82
6.4.3. Design Deficiencies	83
6.4.4. Operating Results	84
7. ACKNOWLEDGMENT	93

LIST OF FIGURES

<u>Figure No.</u>		<u>Page</u>
4.1	Exploded Diagram of Matrix Cell Design	11
4.2	Exploded View of 0.25-sq-ft Acid Matrix Fuel Cell Stack, Original Design	12
4.3	Exploded View of 100-sq-in. Acid Matrix Fuel Cell Stack, Original Design	13
4.4	Design Pattern of Original Bipolar Plate	15
5.1	Design Pattern of Original Bipolar Plate	26
5.2.	Engineering Drawing of Mill Cutter Profile	28
5.3	Engineering Drawing of Die Set	30
5.4	Photograph of Bipolar Plate, New Design	32
5.5	Isometric Sketch of Inlet Orifices	37
5.6	Isometric Sketch of Gas Outlet	39
5.7	Engineering Drawing of Compartment Frame	44
5.8	Photograph of Teflon Compartment Frame (Air Compartment)	45
5.9	Engineering Drawing of Liquid Cooling Plate Frame	58
5.10	Photograph of Partially Assembled and Completed Liquid Cooling Plate	59
5.11	Engineering Drawing of Plastic Insert for Coolant Plate	61
5.12	Components of Air-Coolant Plate	66
5.13	Completed Air-Coolant Plate	67
5.14a	Pattern Drawing of End Plate	71
5.14b	Machining Drawing of End Plate	72
5.15	Photograph of Finished End Plates	73
5.16	Three-Cell Module (Liquid Coolant) on Test	76
5.17	Photograph of 12-Cell Stack (Air-Cooled)	77

Preceding page blank

LIST OF FIGURES, Cont.

<u>Figure No.</u>		<u>Page</u>
6.1	Performance of 12-Cell Stack	85
6.2	Performance of Individual Cells on Hydrogen-Air	86
6.3	Performance of Individual Cells on Hydrogen-Air (IR-Free)	87
6.4	Performance of Individual Cells on Reformed CITE Fuel (2.4% CO) and Air	88
6.5	Expected Performance of 12-Cell Stack Composed of Cells Equal to Average of Five Better Cells	89
6.6	Expected Performance of 12-Cell Stack With Minimized Resistance at Elevated Temperature	90

LIST OF TABLES

Table No.Page

5.1 Pressure Drops for Air Flow

46

1. SUMMARY

The work in this project was a continuation of earlier studies under the same contract number. In the earlier studies, two primary tasks were involved: evaluation of multicell stack performance and operation of a breadboard system consisting of an integrated reformer-fuel cell stack combination. All of the fuel cell stacks in that program were based on existing designs. Those studies were relatively successful, but they illustrated the need for improved mechanical fuel cell and stack design.

The purpose of the studies described in this report was to redesign the existing IGT compact fuel cell hardware, with particular emphasis upon higher temperature operation. This has been successfully accomplished.

The type of fuel cell studied may be classified as -

- Low temperature
- Acid electrolyte
- Constrained matrix
- Reformed hydrocarbon fuel
- Air oxidant
- Liquid cooled
- Employing commercially available, low-noble metal loading electrodes

These cell stacks were quite compact, with 8-10 cells stacked per inch, exclusive of end plates and provisions for cooling.

In the present study, the limitations of the earlier stack hardware were examined in detail. The following attributes were desired in the new design:

1. Compactness. The philosophy of the compact stack, based upon the thin bipolar plate, should, if possible, be extended. Savings in thickness and weight should be possible by redesign of the cell interstage coolers.
2. Use of Commercially Available Electrodes. Although desirable, this point became academic midway through the program when the only commercial electrode supplier discontinued manufacturing this product.

3. Operation at Higher Temperature. Improved stack performance and reduced anode poisoning could be achieved at temperatures of 250°-275°F, beyond the limitations of the earlier stack.
4. Improved Bipolar Plates. Some corrosion of the columbium bipolar plates had been experienced in the earlier stacks, even at the lower temperatures. Improved materials were required, as well as new forming techniques.
5. Improved Matrices. The glass-fiber matrix used in the earlier cells degraded with time, even at the lower temperatures. Greater chemical resistance and bubble-strength were required.
6. Improved Gas Distribution and Pressure Drop. The distribution of both fuel and oxidant gases was occasionally unsatisfactory in the earlier design. Maldistribution across the face of the cell would cause local concentrations of inerts, and poor cell-to-cell distribution would cause excessive drying of some cells with insufficient fuel or oxidant to others. In a related problem, the pressure drop of both gas streams across the stack was excessive. Improved distribution would permit more uniform and reliable cell operation, and the lower pressure drop would reduce matrix breakdown.
7. Improved Gasketing. Slight seepage of electrolyte, fuel gas, or oxidant was a bothersome problem with the earlier cell design, but was not critical in stack operation.
8. Improved Manifolding. All gases and coolants should be internally manifolded in the stack. Internal gas manifolding had been used in the earlier stacks, but improved designs were desirable. The coolant flow in the earlier stack was externally manifolded, causing an array of thermally and electrically insulated piping which should be avoided.
9. Improved Component Strength. The coolant plates and end plates of the earlier design were subject to bulging and warping under excessive coolant pressure, causing uneven cell compression.
10. Component Uniformity. In the previous design, most components were handmade, resulting in nonuniformity. When possible, dies and jigs should be used to ensure standard component structures.

Every component of the fuel cell stack was redesigned to meet these goals. A design philosophy of separation of function was followed. Each component was designed for a particular purpose, rather than combining several functions in one part. This increased the number of components, but simplified each of them.

Primary design emphasis was placed on the formed thin bipolar plate. The IGT bipolar plate concept is the foundation for the compactness of the fuel cell stack.

- The material for the bipolar plate was changed to tantalum for improved corrosion resistance at elevated temperatures. The tantalum was to be gold-plated for minimum contact resistance.
- The thickness of the plate was increased to 0.007 in. for improved strength and dimensional stability.
- The primary wave pattern was deepened for reduced pressure drop and more uniform flow over the face of the cell. The pattern used a rounded form at both peaks and valleys for improved strength and electrode contact.
- Cross-grooves, perpendicular to the primary wave pattern, were incorporated into both sides of the bipolar plates by a secondary embossing operation using mating steel dies. The cross-grooves minimize dead area on both fuel and oxidant sides of the plate.

The gas flow distribution from cell to cell was controlled by incorporation of die-formed orifices as gas inlets to each cell. The orifices were sized for a pressure drop of 2.5 in. wc at design operating conditions; with the improved flow across the bipolar plates, these orifices were the overwhelming pressure loss in the cell, permitting uniform reactant distribution in the stack.

The gas distribution across the face of the cell was controlled by the shape of the compartment frame. The inlet gas, at high velocity because of the orifices, impinged upon the inside edge of the compartment frame. This edge was shaped so that each channel of the bipolar plate received a similar flow of reactant gas.

The gas compartment frames were made of TFE polymer for improved dimensional stability. The thickness of 0.025 in. was optimum for stack resistance and gas flow distribution.

The gaskets between the bipolar plate and the compartment frame were beads of 0.031-in.-diameter peroxide-cured EPT rubber. They were glued into etched grooves in the TFE with EPT rubber cement. The thin beads reduced the stack compression forces required for higher pressure sealing. The gasket beads were located near the outside edge of the compartment frame for reduced bolt-to-gasket distances, improved stress distribution, and reduced end-plate deflection.

The matrices used in the cell stack were a proprietary third-generation, higher temperature material developed by Pratt & Whitney. They had excellent corrosion resistance, dimensional stability, and wet strength. The edges of the matrices were impregnated with Kel-F 800 for self-gasketing to the compartment frames.

The electrodes in the cell stack were made by American Cyanamid Co. The cathodes were Type AA-3 containing 5 mg Pt/sq cm and the anodes were the CO-tolerant Type RA-2, containing 2.5 mg Pt and 2.5 mg Rh/sq cm with amorphous tungsten oxide admix.

The internal gas and liquid coolant manifolds, longitudinal through the cell stack, were formed by holes punched in the edges of the layered components. These manifolds were sized so that the cross-sectional area of the manifolds was a factor of 10 greater than the total area of the outlets from the manifolds. This sizing provides uniform pressure and flow to all outlets from the plenums.

Two types of stack cooling were designed. The first design used liquid cooling plates located every three cells in the stack. The plates, 1/8 in. thick, were made of copper in several components. The parts were tin-plated and the assembly was sweat-soldered into a strong, reinforced hollow unit. Preliminary tests indicated uniform coolant flow. The faces of the coolant plates were protected from corrosion by tantalum sheathing, and the gas-manifold holes were machined Kel-F inserts with Viton O-ring seals to the tantalum.

The coolant manifold gasketing was not satisfactory, so an alternative air-cooling system was developed. This system employs secondary air (rather than reactant air) coolant for independent temperature control and electrochemical operation. The air coolant plates were again located every three cells, but were now 1/4 in. thick for reduced blower power requirements. The thicker air plate, however, weighed less than the liquid plates with the coolant inventory. They were also made from sweat-soldered tin-plated copper. The reinforcement between the faces of the plate was Twin-fold copper, acting as heat-transfer fins. The air was not internally manifolded; rather, a plenum at one edge of the stack supplied the air to the individual plates.

The end plates were designed for reduced deflection under load. They were solid cast aluminum, with flat faces for compressing the stack and a honeycomb bridgework for maximum strength. The gas inlet and outlet plenums were fed from the end plates using machined Kel-F inserts to protect the aluminum from acid attack.

The stack was compressed by external tie-bolts. The compressive force of the bolts was transmitted to the opposite end plate by calibrated die-springs so a controlled loading was possible.

In general, all of the design criteria stated earlier were met or exceeded in the present program, with few exceptions. These exceptions were -

1. Satisfactory internal manifolding of the silicone cooler was not accomplished because of gasketing problems; however, the contract was modified to substitute air-cooling which was satisfactorily accomplished.
2. Tantalum metal is a satisfactory material for the bipolar plates if it is gold-plated for minimum electrical resistance, but the only supplier capable of plating the tantalum quoted a prohibitive price, so this component was not plated in the stack.
3. After routine resoaking maintenance, the excess electrolyte could not be readily expelled from the cells, causing cell-to-cell gas maldistribution.

This design project may now be academic with the discontinuance of the commercial American Cyanamid electrodes. Yet, the compact hardware offers several engineering advantages, and it might be satisfactorily mated to the Engelhard electrode-matrix package. As these electrodes are nonweeping, electrolyte inventory should not be a problem; the difficulty experienced with rewetting the matrix with electrolyte would be avoided. Similarly, tantalum metal would not be required for corrosion resistance. High-grade stainless steel bipolar plates could be readily gold-plated for reduced resistance and current removal. Perhaps an additional layer of fine screen would be required between the electrode and the bipolar plate because of the higher resistance of the Engelhard electrode and the relatively wide spacing of the ridges of the bipolar plate. We recommend this course of action to the Sponsor in its continued use of this hardware.

2. OBJECTIVE

The objective of the work under this contract extension was to redesign the existing IGT compact acid fuel cell stack, which uses commercially available electrodes, to permit higher temperature operation with improved reliability and performance.

3. INTRODUCTION

3.1. History

3.1.1. Initial Work

The Institute of Gas Technology was engaged in fuel cell research in the late 1950's. Extensive research has been conducted on high-temperature molten carbonate fuel cells to operate on natural gas. In 1963, IGT started a second major fuel cell program based on low-temperature acid fuel cell concepts.

The acid fuel cell is attractive because of its tolerance for CO_2 in the fuel and air streams. However, a low-temperature, direct methane fuel cell was not likely to be economically successful. A three-stage chemical process was developed that produced hydrogen from natural gas. This gas was then used for fuel for the low-temperature acid fuel cell. Because of the relative simplicity of the hydrogen generator for acid fuel cells, and the resultant overall system simplicity, this approach has been considered to be an attractive hydrocarbon-consuming fuel cell system even though present performance and cost characteristics might be inferior to alkaline fuel cell technology because the problem of carbonate formation is avoided.

IGT's first experience with acid fuel cells was with dual-ion-exchange membrane fuel cells. Development of this type of cell was abandoned, however, in favor of the constrained matrix type of cell that appeared to hold greater promise with respect to ultimate cost reduction.

Initial investigations with immobilized electrolyte or matrix fuel cells (cells having no free electrolyte) indicated that higher power densities may be obtained and that lower cost electrodes might be employed. Accordingly, battery stacks with immobilized electrolytes were built and operated. Many hours of operating time were accumulated in investigating control variables and scale-up factors.

The technology progressed from high-cost, hydrogen-oxygen batteries to more moderate cost units operating on reformed natural gas and air.

In addition to the program to develop the fuel cell batteries, investigations of the reforming of natural gas and liquid hydrocarbons to produce satisfactory fuel cell feeds have also been conducted at the IGT laboratories. Work on the low-temperature (850⁰-1050⁰F) reforming of liquid hydrocarbons has been particularly successful.

3.1.2. Earlier Work Under This Contract

The initial work by IGT for the U.S. Army Mobility Equipment Research and Development Center in Fort Belvoir (then the U.S. Army Engineer Research and Development Laboratories) was started under the present contract number on October 13, 1966. That project was divided into two tasks: a) Evaluation of Multicell Stack Operation and b) Operation of a Breadboard System consisting of an Integrated Reformer-Fuel Cell Stack combination.

Over 6300 hours of stack testing time were accumulated on phosphoric acid, matrix fuel cell stacks with individual stacks operating to lifetimes of 1250 hours. These stacks were operated at temperatures of 200⁰, 250⁰, and 300⁰F on fuels containing 0.2% carbon monoxide (a possible product from a liquid hydrocarbon reformer and shift reactor) and 3.0% carbon monoxide (a possible product from a low-temperature liquid hydrocarbon reformer alone). Anodes containing 9, 5, and 2 mg noble metals/sq cm were tested during the project. Cathode loadings were 9 and 5 mg platinum/sq cm.

Life-testing was successful at 200⁰F; similar tests at 250⁰ and 300⁰F were not as satisfactory because of matrix degradation and metallic corrosion. The primary routine maintenance required was replenishment of the acid electrolyte.

An integrated low-temperature reformer-fuel cell stack operated satisfactorily during a 100-hour feasibility test run, with a total electrode loading of 10 mg noble metals per sq cm and performed well on the reformer product gases containing 64% hydrogen and 1.7-3.5% carbon monoxide.

Lead removal was satisfactory on synthetically doped gasolines (at 2.5 cc TEL/gal). Conventional cobalt-molybdenum catalysts were satisfactory for removal of 1000 ppm of thiophenic sulfur from kerosene and gasoline fractions. The low-temperature reforming catalysts operated satisfactorily in the temperature range of 900⁰-1000⁰F, producing a fuel containing 1.7 to 3.5% carbon monoxide.

One of the primary difficulties observed during this previous testing program was the mechanical configuration of the fuel cell stack. The earlier program was based on cell designs that were available at the beginning of the program, and the test work defined some of the deficiencies in those cells.

The reader is specifically directed to earlier reports by IGT to USAMERDC under contract number DAAK 02-67-C-0063 for complete details on this earlier test work.

3.2. Present Program

The present program was a logical outgrowth of the earlier work. The earlier program had indicated two avenues for continued research: improved stack hardware and development of better preconditioning for the fuel cell feed. In the field of feed pretreatment, USAMERDC turned its attention from the more complex system of liquid hydrocarbon reforming to the simpler, but less efficient, system of hydrocarbon cracking for producing hydrogen-rich fuels. Indeed, IGT participated in that program under contract DAAK 02-69-C-0452 in which we successfully operated a thermally regenerative, noncatalytic pyrolysis unit for the thermal cracking of gasoline to hydrogen-rich fuel.

The other primary path for development was improvement of the fuel cell hardware. IGT had the requisite stack operating experience and engineering capability for this effort. This background complemented the American Cyanamid capability for the manufacture of fuel cell catalysts. Therefore, a workable fuel cell should be possible using a combination of these talents.

Accordingly, the present project was evolved. The primary aim in the project was to improve the mechanical design of the fuel cell stack to permit improved reliability and operability. Also, the stack should be operable at higher temperatures that would permit improved cathode performance, reduced anode poisoning by carbon monoxide, and potentially lower loading electrodes. The same general type of fuel cell was to be employed: low temperature, constrained matrix, immobilized phosphoric acid electrolyte, reformed hydrocarbon fuel, air oxidant, liquid cooled, and employing American Cyanamid electrodes. Larger cell areas of approximately 100 sq in. were desirable, and the resultant battery stack had the goal of 350 watts at 7 volts output. Additionally, this stack should be operated at loads varying from 5 to 100% of rated current, and routine maintenance procedures should be checked.

3.3. Contract Modifications

Late in the contract, difficulties were experienced in sealing the internal manifolding of the hot (300°F) silicone stack coolant with available elastomeric gaskets. Modification of the existing stack coolant plates to external manifolding was also unsatisfactory because of high pressure drops involved in the associated manifold piping. The Sponsor agreed that air-cooling of the cell stack would be more desirable considering the ultimate intended use of the power source. Therefore, the contract was modified to extend the design to air-cooled stacks. Air-cooling was to be supplied separate from the cathode air for improved moisture balance and temperature control. Cells were to be cooled in groups of 2-6, depending upon the cell-to-cell temperature variation experienced because of the conduction through the cells to the coolant plates.

3.4. Future Work

Midway through the test program, American Cyanamid discontinued the manufacture of fuel cell electrodes. Other manufacturers were generally reluctant to release the control of their electrodes. Therefore, the developmental work on these stacks was terminated when the available supply of Cyanamid electrodes was exhausted.

We believe that the development to date indicates sufficient promise that the Sponsor, with his contacts with other electrode suppliers, can exploit the IGT design concept and develop superior fuel cell hardware.

4. PREVIOUS DESIGN

Because the redesigned fuel cell stack feeds upon the earlier equipment, that earlier design — its origin, growth, and limitations — will be reviewed first.

Figure 4.1 is an exploded diagram of the matrix cell design.

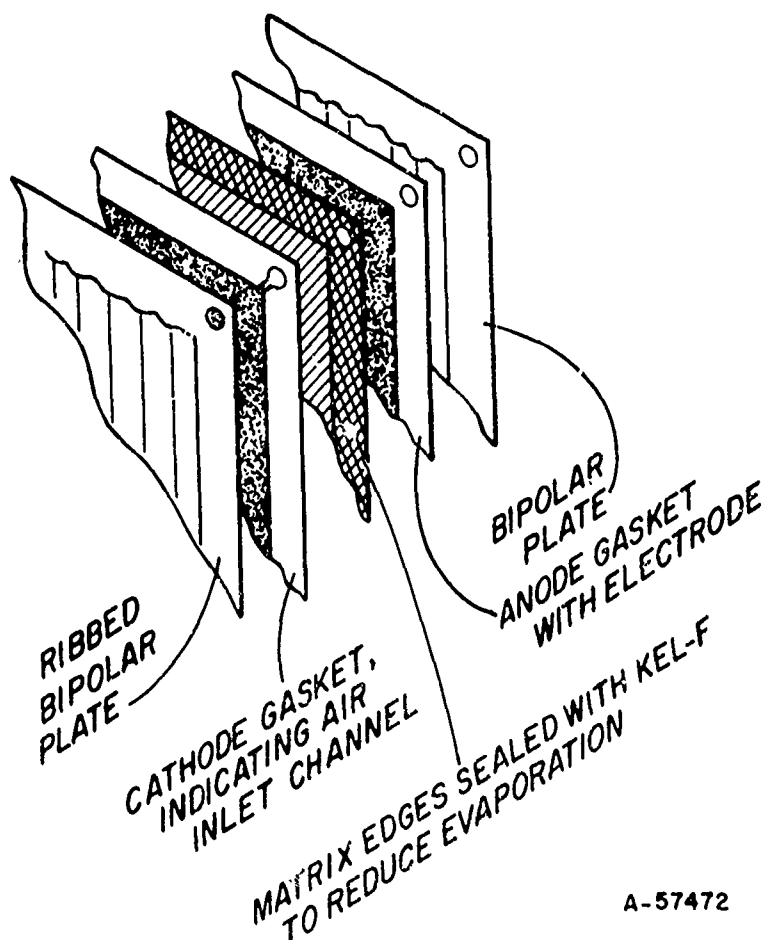


Figure 4.1. EXPLODED DIAGRAM OF MATRIX CELL DESIGN

The cell is constructed in layers in a technique that could, eventually, be adapted to mass production. Each of the layers is quite thin, permitting a compact cell which is less than 1/10 in. thick. The center layer of the cell is the matrix which retains the immobilized phosphoric acid electrolyte. Adjacent to and on either side of the matrix are gaskets

with an open area in the center for the American Cyanamid electrodes. The gaskets seal against the matrix edge, and the electrodes contact the acid on either side of the matrix. External to the gaskets are the ribbed bipolar plates. These thin plates have a series of ribs and cross-grooves to hold the electrode against the matrix, to withdraw the current from the electrode, to distribute the reactant gas, and to transfer the current to the adjacent cell. Figure 4.2 is a photograph of a disassembled cell in a 0.25-sq-ft stack.

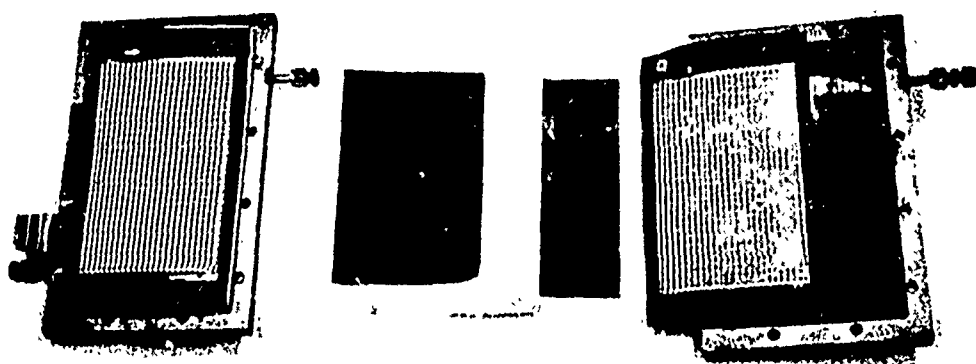


Figure 4.2. EXPLODED VIEW OF 0.25-sq-ft
ACID MATRIX FUEL CELL STACK, ORIGINAL DESIGN

The ribbed bipolar plates for each side of the cell are shown on the end plates (which double as cooling plates). The gaskets are shown in place on the bipolar plates, forming anode and cathode fuel compartments. The white matrix in the center of the picture is flanked by the two electrodes which form the heart of the fuel cell. A similar photograph of a 100-sq-in. fuel cell is shown in Figure 4.3, which illustrates the larger hardware involved.

The individual components in this stack will be discussed in detail later.

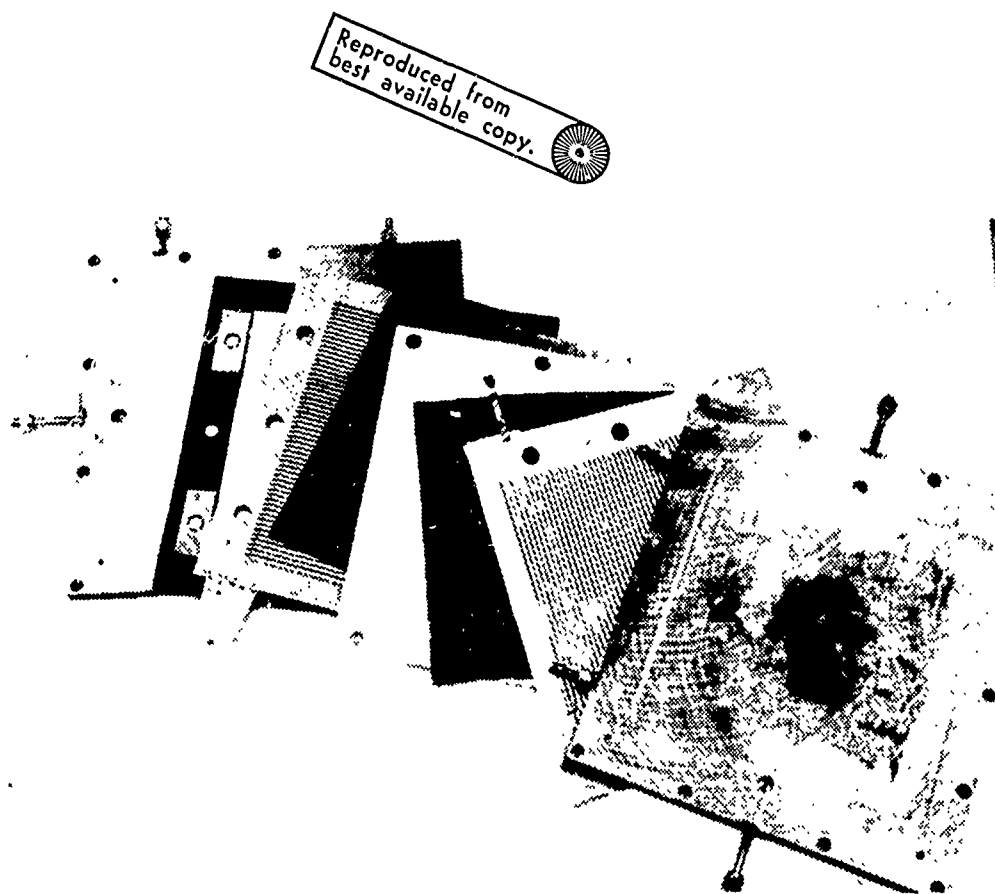


Figure 4.3. EXPLODED VIEW OF 100-sq-in. ACID MATRIX FUEL CELL STACK, ORIGINAL DESIGN

4.1. History

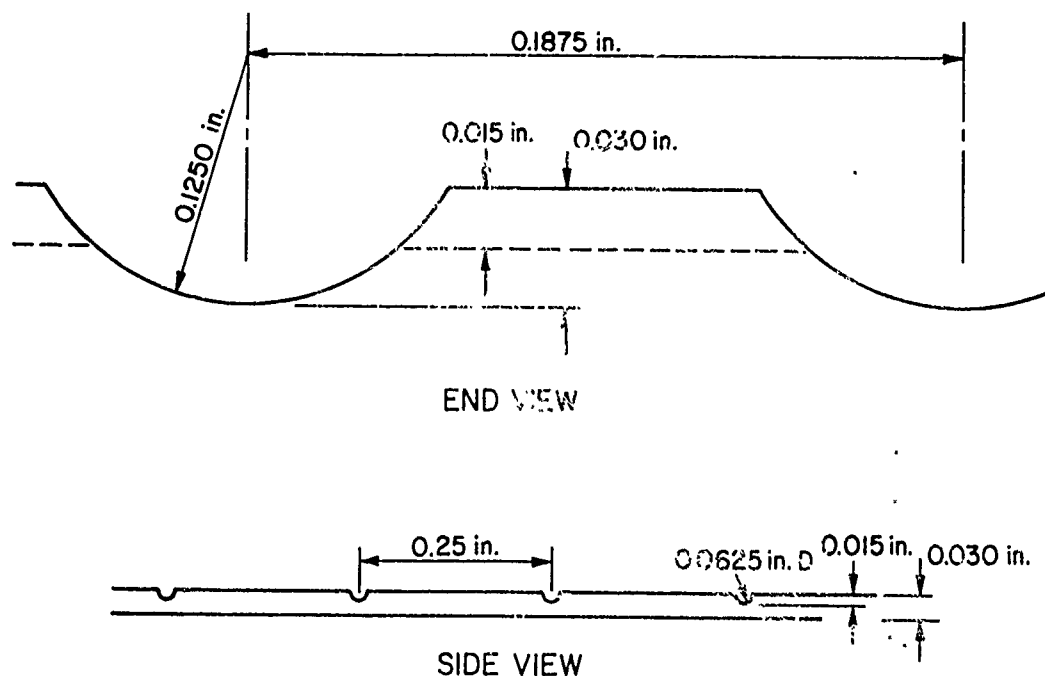
The history of the IGT matrix stack hardware traces to the dual-ion-exchange membrane fuel cells that were first tested in a gas-industry program at the IGT direct-energy conversion laboratories in 1963. These cell stacks operated first at 60°F and then up to 150°F with a sulfuric acid electrolyte. The sulfuric acid was circulated through the cells for control of both acid concentration and stack temperature. Thin compartments of electrolyte in each cell were bounded by an ion-exchange membrane which permitted the transfer of hydrogen ions from the anode to the electrolyte and from the electrolyte to the cathode. These cells used internal manifolding of fuel, oxidant, and electrolyte. Gas compartment frames were made of Teflon with extremely thin rubber gaskets between

the Teflon and the ion-exchange membranes and between the Teflon and the bipolar plates. The bipolar plates were simple flat sheets, and spring-tabbed current collectors were used to hold the electrode against the ion-exchange membranes, withdraw the current from the electrodes, and transfer it to the bipolar plate. Because of the corrosion problems, only columbium or tantalum were satisfactory constructional materials; columbium was chosen because of its lower price on a volumetric basis. Gas distribution from the internal manifolds (larger holes longitudinal in the cell stack) to the gas compartments were small holes drilled in the thickness of the Teflon compartment frame between the two zones.

As higher currents were drawn and air was substituted for oxygen in the cells, the holes in the Teflon became restrictive and were replaced with slots cut between the manifold hole and the gas compartment. Similarly, when the hydrogen was replaced with reformed hydrocarbons, the anode drilled hole was replaced with a slot containing a calibrated length of tantalum hypodermic tubing for better cell-to-cell distribution.

At this time, the bipolar plates evolved. The three-layered current collector and bipolar plate combination was replaced with a ribbed structure. The ribs were generated by squeezing the fully annealed, ductile columbium sheet between a constrained 60 durometer polyurethane molding block and a premachined die. This die was constructed by cutting parallel grooves, 0.030 in. deep, with a 1/8-in. ball-end mill on 3/16-in. centers in the area of the gas compartment. The die was relieved 0.015 in. in the area of the gasketing, and cross-grooves of that depth were cut perpendicular to the main grooves with a 1/16-in. ball-end mill on 1/4-in. centers to yield the design pattern indicated in Figure 4.4. This is the basic design of the bipolar plate used in all of the earlier matrix cell studies.

When properly annealed, thin sheets pressed in this manner formed a series of gas distribution grooves on either side of the bipolar plate. One side had slightly larger grooves, but no cross-connections; this side was used for the air flow because of the greater volumes required. The cross-connections minimized dead area and resultant CO poisoning on the anode side of the plate.



A-32266

Figure 4.4. DESIGN PATTERN OF ORIGINAL BIPOLAR PLATE

Specification of the columbium sheet was important. The material must be fully annealed so that it would not unduly work-harden and crack, causing hydrogen-oxygen mixing in adjacent cells. Of the various suppliers tested, the best material came from the Haynes Stellite Division of Union Carbide, followed by Kawecki Chemical, and then Fansteel Co.

The thickness of the sheet to be pressed was also important. Insufficient force was available, even for small 1/4-sq-ft cells, from the IGT 200-ton hydraulic press for satisfactorily deep impressions on 0.015-in. material, which was desirable for current removal rates. At a minimum material thickness of 0.005 in., the impressions were sharp but the rejection rate was relatively high because of work-hardening and stress cracking. A compromise of 0.007 in. was reached. An aluminum backing sheet was resistance-welded to the current removal pads for minimum voltage drop in the end monopolar plates.

Later in the program, when larger cells were manufactured, a Hydroforming technique was used to form the plates. This equipment uses high-pressure oil behind a thin rubber sheet which compresses against the columbium sheet stock and the die. Very high unit pressures are possible. Clearly defined plates were made by this technique on the 100-sq-in. bipolar plates.

With the ribbed bipolar plates, new compartment frames were required because the available ridges were only 0.015 in. above the neutral surface of the plate. Butyl rubber of 1/32 in. was used satisfactorily. Later cells used Ethylene-Propylene (EPT) rubber for better chemical resistance.

The same basic cell design was carried over to the first of the matrix cells. In this case, the recirculating electrolyte compartment and the ion-exchange membranes were replaced by a thin matrix with a gasket. Later, IGT patented a technique for impregnating the edge of the gasket with Kel-F that effected a seal against the frame compartment gaskets and eliminated a potential cross-leakage problem. Also, this technique helped to constrain the electrolyte within the matrix and avoided leakage problems from the cell.

The distribution of the gas from the manifolds to the compartments also received attention. On the fuel side of the cell, the angle of the hypodermic restrictor was altered with significant improvement in cell performance. Eventually, the needle was omitted, and the gas slots from the manifolds to the compartments became wedge-shaped openings, first of 45 degrees and later up to 90 degrees included angle. The Kel-F impregnated matrix tended to extrude into these wider openings so small tabs of columbium sheet metal were placed between the matrix and the frame compartment in these areas.

In the larger cells, two gas inlets and one outlet were provided for each cell in order to minimize the distance the gas would have to travel across the top or bottom of the cell. This technique improved the gas distribution.

The structural end plates of the original IEM stacks had been constructed of 1/2-in. Hastelloy C (for corrosion resistance against the sulfuric acid at the electrical potential). With the advent of the matrix cell, stainless steel was substituted. Corrosion was still experienced

at the gas inlets and outlets because of electrolyte seepage. Kel-F plugs were inserted into the plates in these areas to eliminate the acid attack. Temperature control was provided by heaters on the face of these end plates. However, as the stacks grew larger, better temperature control was required and the 1/2-in. stainless end plates were machined hollow for recirculation of glycerine or silicone coolant. A multiple-pass coolant system was effected with 3/8-in. square rods in the hollow end plates. The faces of the coolant zone were 1/16-in. stainless sheets which were welded to the end-plate frame and resistance-spot-welded to the flow-separating rods. The face of the end plate was then surface-ground for flatness. Tubing for the coolant flow to the stack entered through the edge of the plates.

This history updates the cell design through the earlier program. The various cell features can be noted in the photographs of Figures 4.2 and 4.3.

4.2. Deficiencies of Previous Design

Deficiencies of the earlier design have been enumerated in earlier reports of this project. These deficiencies are summarized below for reference in the evolution of the new cell design. The problems associated with the attainment of the maximum performance of the earlier cell can be categorized into three areas: materials of construction, cell design, and manufacturing techniques.

4.2.1. Materials of Construction

Improved fuel cell operation could be obtained in the temperature range of 250⁰-300⁰F. Yet, two of the primary constructional materials in the earlier fuel cell showed rapid degradation at these temperatures.

The most severe problem was the material used for the matrix. The best available material was a nonwoven glass-fiber filter-paper mat. This matrix material lost its structural integrity at higher operating temperatures and became a gel, similar to silica gel in character. In the gelled form, the matrix had little strength and would rupture, even with low-pressure differentials between the anode and cathode gases.

The problem with the glass-fiber mats had been experienced at many laboratories, and a number of possible solutions were proposed. One purpose of the present program was to evaluate these proposals and select the most desirable available matrix material.

The metallic components of the earlier cells were made of columbium metal because of its cost advantage (volumetric basis) over tantalum. The columbium was apparently attacked under some cell operating conditions, particularly at higher temperatures. In many instances, a bright blue film was found on the columbium bipolar plates after extended stack testing. This film was not readily removed except by scouring. A more serious problem was the occasional production of an amorphous, white deposit in the grooves of the columbium bipolar plate. This material was not characterized, but initial investigations indicated that it might be a high phosphate of columbium. This deposit was bulky and blocked the gas flow passages within the cell. Again, the generation of this deposit was a temperature function, indicating that columbium could not be used at the desired operating temperature.

4.2.2. Design Problems

As indicated earlier, the previous work under this contract had been done with cells of an existing design. That design had "just grown," incorporating features which had been satisfactory under earlier operating conditions but marginal when advanced operating parameters were used.

The manifestations of the design limitations were —

- a. High pressure drop for gas flow of both fuel and oxidant across the cell.
- b. Apparently unsatisfactory gas distribution over the face of the cell as evidenced by significantly decreased performance at gas flows that were low multiples of the stoichiometric requirement.
- c. Improper cell-to-cell gas distribution within the stack as evidenced by varying cell performances as gas flow rates were reduced.
- d. The forces required to seal the cell edges were occasionally high, causing bowing of the end plates, insufficient bipolar plate-to-electrode contact, and high internal resistance.

- e. The recycling silicone oil coolant system was unsatisfactory. High pressure drops in the coolant end plates caused bulging of these plates and improper intercell contacting. In addition, the external manifolding of the coolant plates was awkward.

The primary problem with the coolant end plates was the high volume of coolant required for isothermal cell operation. This flow rate, in combination with the tortuous flow path and insufficient outlet tubing size, caused high internal pressures in the cooling plates. The metal skin over the cooling zone was not strong enough to withstand this pressure. In addition, insufficient resistance-welding was used to retain this metal in the center of the cooling section. The combination of these factors caused the bulging of the coolant plates.

The bowing of the end plates because of high stack-compression forces is more complicated. The individual cells were sealed around the gas compartments by the full thickness of the rubber compartment frame. This frame had a width of 1 in. around the outside of the electrode area, so relatively high compression forces were required for even modest gasket compression pressures. For example, the 100-sq-in. cell had 44 sq in. of gasketing. At a nominal 100 psi pressure, 2.2 tons of end-plate load were required.

The space between bolts and the gaskets was excessive in the earlier design; sufficient room had been allowed to eliminate the possibility of short circuits from bipolar plates to the tie-bolts. This wider spacing increased the loads necessary in the cell. These resultant forces caused a constrained beam problem, which forced a significant deflection of the 1/2-in.-thick stainless steel end plates at the center of the cell. The problem was accentuated when the stainless plates were hollowed for coolant passage.

The problems of pressure drop and gas distribution are interrelated in the design of the bipolar plate rib pattern, the gas inlet slot, and compartment frames. In the earliest designs, these problems had not appeared because of the use of pure gases. With the substitution of impure and catalyst-poisoning gases on single cells, the distribution problem across the face of the cell became more noticeable. Techniques that had proved applicable to the smaller, 1/4-sq-ft cells were applied to the large cells and found to be usable, if not entirely satisfactory.

Cell-to-cell maldistribution was also not evident with pure gases or higher flow rates and had not been expected because of the supposed uniformity of the cell construction. Similarly, high cell pressure drop was not a problem with pure gases or with strong matrices, but it became an undesirable cell characteristic at higher operating temperatures or longer cell life when matrix degradation had occurred. This pressure drop was probably caused by insufficient rib depth. Blocking of gases' inlet and outlet passages (slots cut in the rubber compartment frames and protected from the matrix by sheet columbium) was a possible cause because of the high total force on the area of the open slot, even if somewhat protected from blockage by the sheet columbium. This gas passage blockage could also account for both types of gas maldistribution. Similarly, flattening of the ribbed bipolar plate under the compressive load could cause gas distribution problems. However, although often suspected in stack operation, no clear evidence of this phenomenon occurring was found.

4.2.3. Manufacturing Techniques

All of the components of the fuel cell stack were made by hand, with resultant tolerances in manufacture. Slight variation in the Hydroforming pressure would cause differences in the depth of the grooves of the bipolar plates. Similarly, the holes and slots in the compartment frame gaskets were not absolutely uniform. These manufacturing techniques contributed to the gas distribution problems which occurred at lower feed rates of dilute fuel and oxidant.

5. NEW HARDWARE DESIGN

Every component of the fuel cell stack was redesigned. This section details the design of each component as well as the factors used in selecting that design.

5.1. Design Philosophy

The primary consideration in the redesign of the fuel cell stack was improved operability. The possible factors that caused the operating problems in the previous stack design were evaluated and eliminated in the new design.

The second primary consideration in the stack redesign was compactness and minimum weight. The compactness was a desirable attribute in the earlier design, and we attempted to retain it. It was primarily achieved because of the concept of the thin bipolar plates. The resultant new stack design was even more compact than the previous design. The concepts of compactness and minimum weight are complementary. Weight savings were a result of the compactness. However, in this prototype design, weight was not considered a critical design factor. For example, we used copper in the cooling plates for ease of manufacture where aluminum might be substituted in a production cell, with significant weight savings. Similarly, the end plates were sand-cast in aluminum where magnesium might be used if weight savings were desirable. Also, the end plates could be redesigned to use less material if beryllium alloy with high elastic modulus could be used. These factors, however, were believed to be incidental to the primary function of building a prototype cell stack.

A major design philosophy was the separation of functions. For example, the earlier design used sheet EPT rubber as a combination of compartment frame and gasket material. The new design uses Teflon for the compartment frame for greater mechanical stability with a thin bead of EPT rubber as a gasketing material. Similarly, the end plates and cooling plates were each designed for a specific function.

5.2. Bipolar Plates

The compact cell design concept hinges on the satisfactory use of the thin bipolar plate. The bipolar plate serves many functions (which cannot be separated into individual components according to the design philosophy above without adding complexity and probable loss of operability of the cell). The bipolar plates remove the current from the electrode of one cell and offer a low electrical resistance path for the flow of this current to the other electrode of the adjacent cell. One side of these plates forms distribution channels for the supply of fuel to the anode of one cell, and the reverse of the plate forms channels for the supply of oxidant to the cathode of the adjacent cell. In its simplest sense, the bipolar plate is a series of ridges and valleys embossed in the sheet metal within the electrode area of the cell. A ridge on one side of the plate becomes a valley on the other. Similarly, cross-grooves may be incorporated to minimize the dead area within the cell.

The bipolar plate must have structural integrity to avoid the mixing of the oxidant of one side with the fuel on the other. Similarly, it must be strong enough to transmit the compressive forces within the cell area throughout the length of the cell stack so that good plate-to-electrode-to-electrolyte contact is maintained. Similarly, it must not significantly deform and flatten under the loading, or the electrode area will be inaccessible to the reactant gases and the gas flow channels will be reduced in volume. These criteria suggest a sharp V-shaped configuration for the peaks and troughs. However, this configuration would offer only line contact with the electrode, with resultant high internal resistance. Similarly, this shape might tend to cut the matrix and would be difficult to produce in the metal without jeopardizing its structural integrity. Arguments and considerations such as the above were used in determining the design of the bipolar plates.

5.2.1. Constructional Material

The number of metallic materials that can be used for the construction of the bipolar plates is quite limited. They must be chemically resistant to the attack of the concentrated phosphoric acid under the electrical potential, both anodic and cathodic, of the fuel cell. Previous studies have indicated that columbium and tantalum were satisfactory constructional materials for this duty, but earlier experience indicated that the columbium was not applicable at the higher temperature of operation (Subsection 4.2.1). Additionally, there was some evidence that the columbium bipolar plates had been flattening in operation because of compressive forces. This might have been because of the design of the ridge-valley pattern used in the earlier cell, but we nevertheless investigated a number of high-tantalum alloys to determine if a corrosion-resistant material might be available to counteract this tendency. For example, the alloy of 10% tungsten in tantalum causes a significant increase in the hardness of the material (with resultant increase in the difficulty of forming). However, none of the commercially available alloys investigated showed a significant increase in the Young's modulus, the primary property which would minimize deformation. The Young's modulus of tantalum is nearly double that of columbium, providing increased resistance to deformation. The slightly increased stiffness (over tantalum) of the harder alloys was not considered worth the effort required to test for corrosion resistance in the difficult fuel cell environment. Therefore, we reverted to the choice of tantalum as the primary metal in the cell stack.

Tantalum, however, has a tough oxide film with a high resistance to electricity. This film is probably the reason for its corrosion resistance. At the beginning of the program, we were assured by a supplier that the tantalum could be satisfactorily plated with gold by a proprietary process so that the plates would have the low contact resistance of the gold with the corrosion resistance and lower cost of the tantalum. But when the bipolar plate design was fixed and the tantalum plates had been manufactured, the price for 0.00005 in. of gold plating finally quoted by the supplier was such that these plates could have been manufactured out of solid gold for less money. The project budget could not afford this

expense, so the decision was made to eliminate the gold plating and to report the stack performance on both net and IR-free basis, indicating the output that could be possible with minimum contact resistance.

We knew, however, that a stack with satisfactorily low resistance could not be built of tantalum without the gold plating. Therefore, we learned techniques for plating tantalum during an in-house project. The tantalum is first flash-plated with palladium in a molten KCN-NaCN bath at slightly above the melting point of the eutectic. An adherent, coherent film is readily obtained at reasonable current densities. The palladium flash serves as a base for the gold plating, which is readily accomplished from a conventional aqueous process. The resultant gold plate is also coherent and adherent and does not appear to lose its attributes as either anode or cathode in water electrolysis at 250°F in phosphoric acid. However, the cyanide plating treatment causes brittleness (perhaps case hardening) in the thin tantalum sheet. We expect that this hardening could be relieved by conventional high-vacuum tantalum annealing techniques. This was not attempted because the cost of the equipment necessary for the larger molten cyanide baths prohibited its use in this project.

5.2.2. Bipolar Plate - Embossing Pattern

The ribbed pattern in the bipolar plate had previously been generated in the columbium sheet by pressing this sheet between a machined die and a deformable polyurethane plastic block. For the larger cell sizes, when insufficient forces were available from the 200-ton press at IGT, the sheets were pressed in a Hydroforming machine that uses high-pressure oil behind a thin diaphragm on top of the sheet and the premachined die. Much higher unit pressures are available using this technique.

The bipolar plates formed in this manner are "embossed": The metal is stretched into the desired shape. We have found that it was important to stretch the metal, rather than draw the metal into the grooves from the side of the sheet because drawing would produce a wrinkling in the flanges of the plate and cause cell sealing problems.

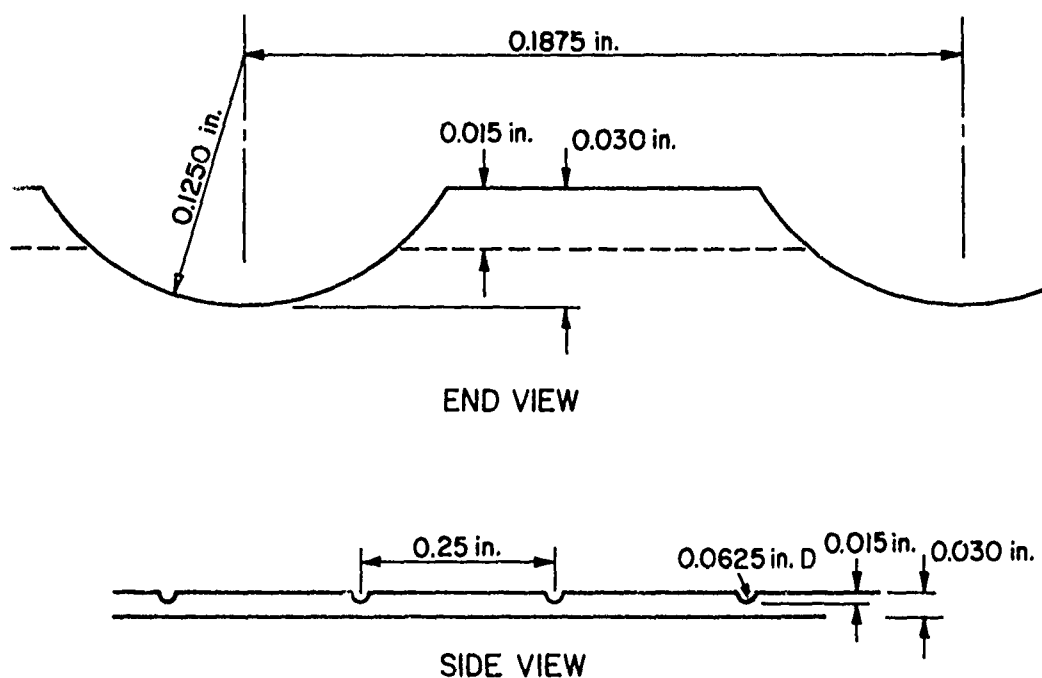
This embossing technique is based upon the ductility of the annealed sheet metal. The material is actually stretched as it is forced into the grooves of the machined die. The depth of the impression is, therefore, a function of the ductility of the metal. If we had pressed lead, which

is dead soft, a clear, sharp impression could be made. Conversely, a glass-hard material could not be formed by this technique. The ductility of the columbium or tantalum is a function of the annealing process which it undergoes after being rolled into sheet stock. As discussed earlier, the most ductile material was obtainable from Haynes Stellite Division of Union Carbide Corporation.

Both columbium and tantalum are subject to work-hardening. As the material is worked or deformed, its microcrystalline structure is rearranged such that it becomes harder: Increased forces cause a spring-like action and when the load is removed, the material will partially recover its original shape. The action is similar to the work-hardening of soft copper tubing. This bends easily the first time it is worked, but resists additional bending with a spring-like action. With increasing work, the copper becomes hard enough to break. The same action occurs in the manufacture of the ribbed bipolar plate out of columbium or tantalum and must be considered in the design of the ribbed surface. The tantalum sheet will work-harden as it is pressed. Although it may completely fill the die during pressing, it will spring back slightly when the load is removed.

The thickness of the tantalum sheet which was chosen for the bipolar plates was 0.007 in. This thickness was arbitrarily selected based on experience with the earlier cells and the ductility of columbium sheet. In that case, 0.005-in. sheet stock was deeply pressed to nearly full die depth but was subject to higher failure rate. Experience with 0.010 and 0.015-in. stock showed imperfect plates because of insufficient impressions. The experience with small cells (0.1 sq ft) and 0.007-in. columbium sheet had been satisfactory, so this thickness was incorporated in the test program.

Figure 5.1 presents the "theoretical" design of the original bipolar plate. In other words, Figure 5.1 presents the design of the female die into which the sheet stock was embossed. With springback due to work hardening of columbium, the embossed depth was approximately 0.028 in. (rather than the 0.030 in. of the die) with 160-ton total force on a 12-in. square sheet. This die provided cross-grooves which permitted cross-flow of the gas on one side of the bipolar plate. Double



A-32266

Figure 5.1. DESIGN PATTERN OF ORIGINAL BIPOLAR PLATE

cross-grooving, permitting cross-flow on both sides of the bipolar plate, was not feasible with a single female die.

The limitations of the earlier design have already been discussed. In brief, the grooves were too shallow, causing high pressure drop within the cell stack. Similarly, these plates were not cross-grooved on both sides, possibly causing dead area on one side of the bipolar plate. There was a possibility that these plates were flattening under load, causing dead area within the cell because of blockage of electrode sites. However, this design provided sufficient information for a satisfactory redesign.

The new design should incorporate deeper ribs for reduced pressure drop. The calculated pressure drop for the cell with the earlier design was much less than actually experienced. Apparently, the electrode and the matrix were extruding into the grooves, causing significant reduction in the area for gas flow. With deeper embossing, the same degree of extrusion will cause a lesser effect on the pressure drop.

The shape of the grooves should be changed for greater mechanical resistance to deformation. The improved Young's modulus of the tantalum should help minimize deformation under load, but rounding of both the peaks and valleys in the plate should give better mechanical strength to resist deformation and minimize dead area within the cell.

The new cell design should have cross-grooves on both sides to minimize dead areas on both anode and cathode of the cell stack.

The inter-rib spacing was satisfactory on the earlier design. Insertion of gold current-collector wire mesh between the electrode and the bipolar plate did not reduce the internal resistance of those cells. Therefore, the same inter-rib spacing of 3/16 in. could be used in the new design.

The first problem was to generate a primary wave pattern for longitudinal gas flow which would be significantly deeper than in the original design. This design must be based on the known stretching and work-hardening capabilities of the metal, but avoid incorporating an additional annealing step in the manufacture. A mathematical study of Figure 5.1 indicates that the overall material length had been increased by 11% in the earlier design (assuming perfect deformation into the die). However, the flat section of the material has not been appreciably stretched; the grooved section of the plate has therefore been stretched approximately 20%. Thus, we should expect to design for a possible 20% elongation of the metal without difficulty. This stretching should result in a slight springback of the deformed piece, significant hardness in the resultant pressed sheet, but not overstretching and failure because of brittleness.

The simplest structure for this type of stretching is a simple V-wave. Mathematical analysis indicates that a nearly 1/8-in. groove depth should be possible. However, this type of design suffered localized overstretching and failure at the points of the female die.

A rounded wave form was tried. A mill cutter was ground to the shape necessary to generate the primary wave pattern in Figure 5.2.

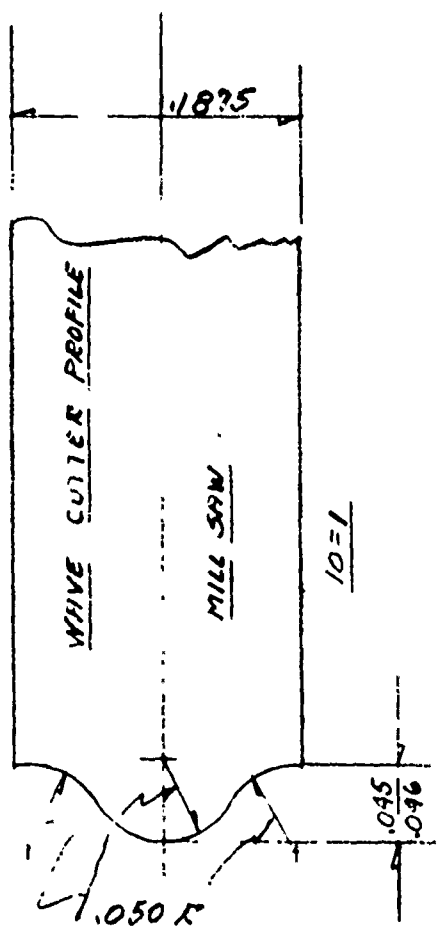


Figure 5.2. ENGINEERING DRAWING OF MILL CUTTER PROFILE

This design used relatively large radii of 0.050 in. (similar to the 0.0625 in. used on the earlier design), and the overall wave depth is 0.045 in. for the 20% stretching of the sheet stock. A die for a 0.25-sq-ft cell was milled in brass with this cutter, and a three-cell stack was constructed with this bipolar plate, but with earlier designs for the other components. The resulting stacks operated well, with low pressure drop. Consequently, this primary wave pattern was used for the design of the 100-sq-in. cell for this project. The cross-groove pattern will be discussed later.

This wave form is not optimized. It is possible to grind other cutters with different shapes, manufacture dies, and build cell stacks to compare performances. However, this design fulfilled its primary goal and provided low pressure drop. Even lower pressure drops were not required in the cell stack, and the evaluation of other embossing patterns was not warranted considering the time, cost, and possible benefits to be achieved.

A steel die was manufactured for the 100-sq-in. cell using this wave pattern. Brass sheets were Hydroformed for mechanical evaluation of the pattern and for flow distribution and pressure drop tests on the larger size. When these tests (discussed in Subsection 5.3) proved satisfactory, an additional steel die was machined to mate with the first die so the embossing patterns could be generated between steel dies on the IGT press (to avoid the time and cost of the Hydroforming). However, the concept of mating dies proved unsatisfactory: The material would draw rather than emboss with this technique of generating the initial waves. However, mating dies were necessary to generate cross-ribs for both sides of the plate. (This is discussed in later in this subsection.) Therefore, the bipolar plates were first pressed on the Hydroforming machine to provide the initial wave form. Then, the plates were repressed between mating steel dies to generate the cross-grooves. Additionally, the steel dies would further deepen the grooves by providing additional forces at the peaks of the hills and valleys.

The cross-grooves were generated by burying wires in the steel dies. Figure 5.3 is the engineering drawing of one of the dies used in this program. A special cutter was ground so that cross-grooves could be made every 1/4 in. across the hills and valleys of the primary pattern. This new cutter would machine a slot that was approximately 0.060 in. across the top, but had a rounded bottom to accommodate a 0.045-in.-diameter piano wire. The cross-grooves in the die were made 0.022 in. deeper than the valleys, and the hardened wires were driven into alternate grooves. In the mating dies, a piano wire at the bottom of the slot in one die would mesh with an open slot on the other die.

A

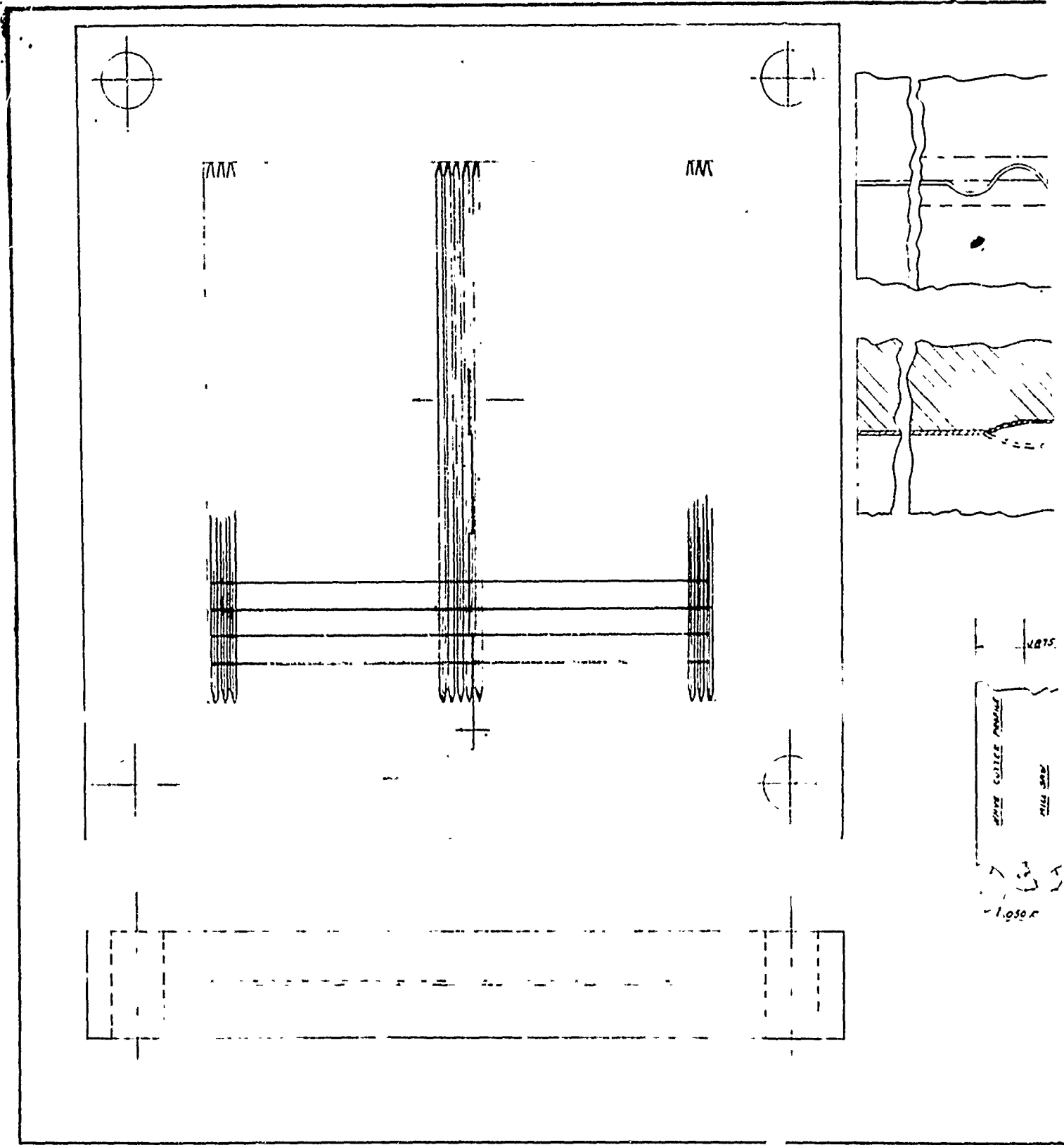
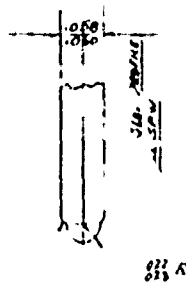
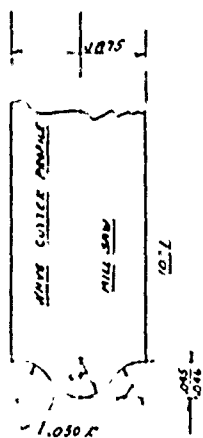
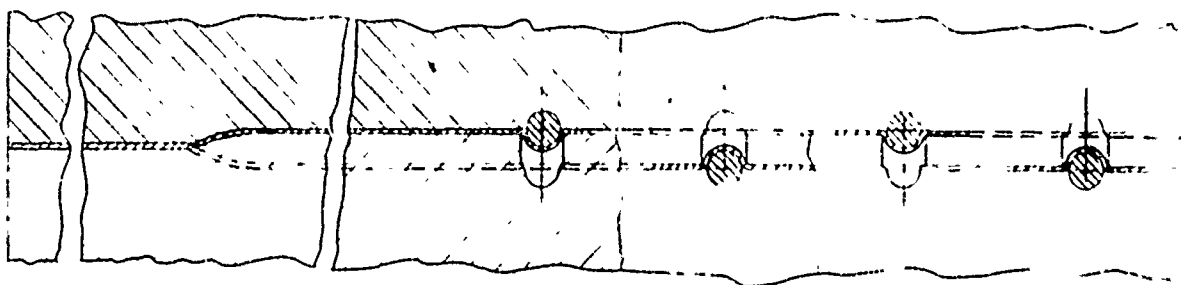
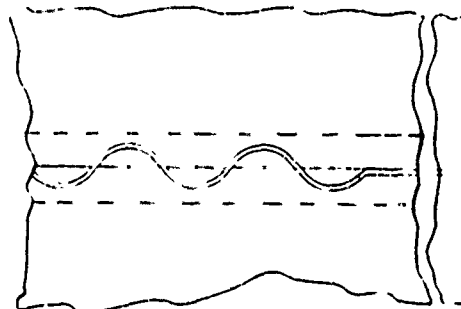
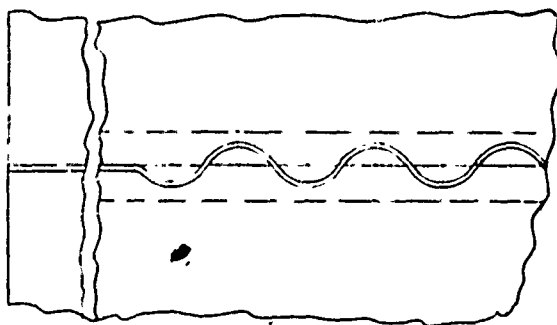


Figure 5.3. ENGINEERING DRAWING OF D

AM



• 010 R
501 N 51563

<div style="text-align: right;">115 7211</div>		
02 00 0 0470 5-68	AUTHORITY: 01	010000 010000 7788 010000
010000 010000		

5. 3. ENGINEERING DRAWING OF DIE SET

A procedure was developed for uniform pressing of the plates. First, the 12-in. square plates were Hydroformed at 7500 psi into a female die without cross grooves. This die had the 0.050-in.-radius hills and valleys on 0.1875-in. center with 0.045-in. depth. The resultant plates were then pressed between steel dies which incorporated the cross-grooves and alternate piano wires at 75 tons total force. The piano wires embossed the metal into the groove on the mating die, but the preformed ridges and valleys did not deform significantly into the cross-groove where no wire was present.

The first plates which were double-pressed with this technique were unsatisfactory. Both dies used a similar wave pattern generated with the same cutter. This caused a pinching of the metal in the flat sections of the wave (near the axis if the wave followed a sine function), locally overstressing the tantalum and causing brittleness and failure. Therefore, one of the mating dies was recut with a new mill cutter which had been ground to 0.057-in.-radius hills and 0.043-in.-radius valleys to allow for the 0.007-in.-thick material. Plates which were double pressed with the new die set were clear and deeply embossed as illustrated by the photograph of Figure 5.4. With this technique, the plates had a uniform overall thickness (including stock) of 0.049 in., indicating a similar springback as experienced in the earlier plates. Of 30 plates pressed in this manner, only two had failures because of pinholes where the cross-grooves met the wave with localized overstretching.

5.2.3. Bipolar Plate — Hydraulic Considerations

Hydraulic considerations are important in the design of the bipolar plate. Ideally, the plates should be uniform in resistance to gas flow so that each cell receives identical quantities of reactant. Practically, however, achieving this uniformity is difficult, and a more logical approach is to incorporate one controllable, overwhelming flow resistance element into each cell. This is the philosophy that was employed in the design of the hydraulics in the bipolar plate.

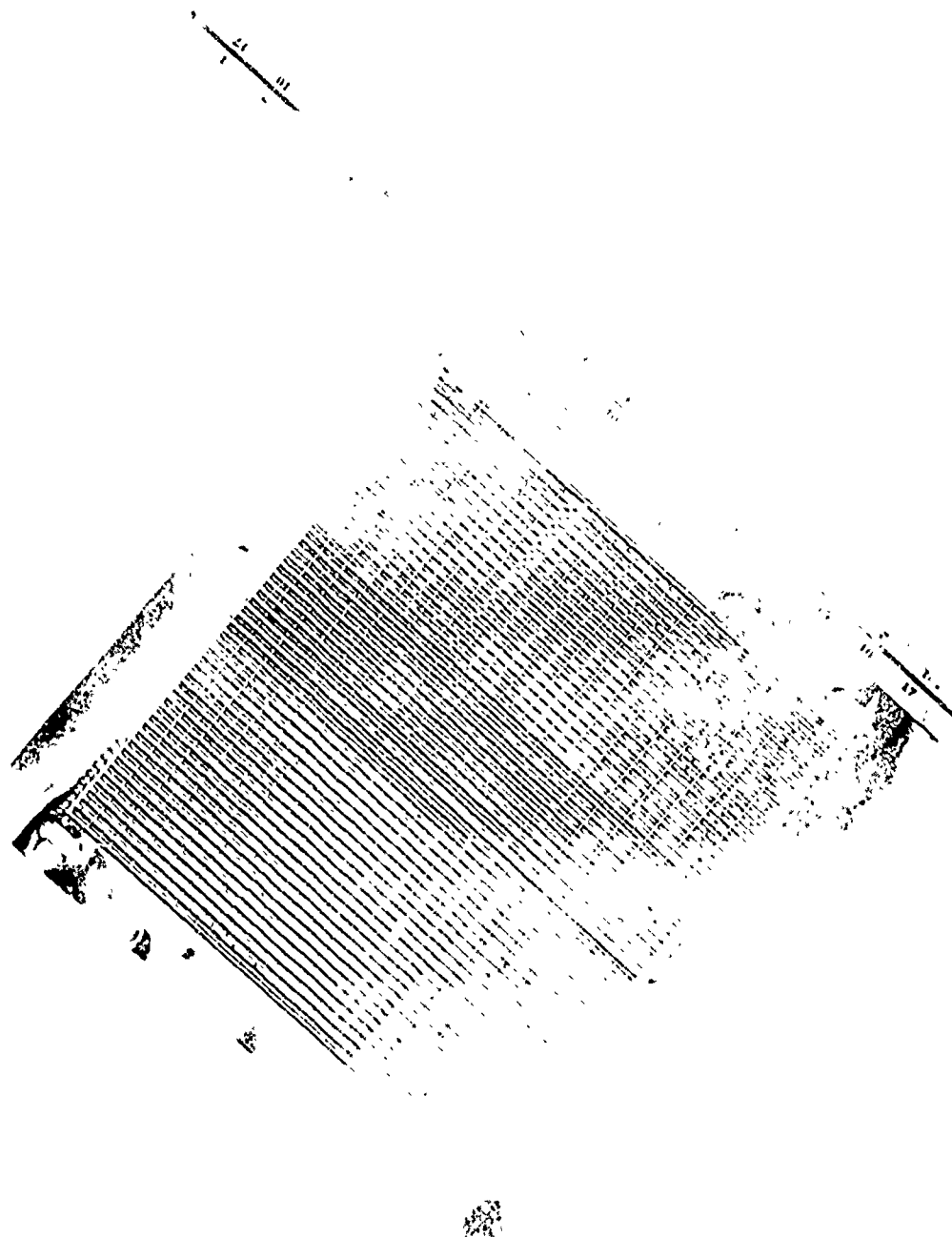


Figure 5.4. PHOTOGRAPH OF BIPOLAR PLATE, NEW DESIGN

The flow of gases may be considered as passing through several pressure drops in series. The first restriction or resistance to flow is the gas distribution manifold in the stack. This manifold is a series of holes punched in the compartment frames, matrices, bipolar plates, and cooling plates. These holes constitute a manifold that runs longitudinal to the cell stack and perpendicular to the face of this bipolar plate. The second restriction is the inlet from this manifold into the gas compartment of an individual cell. The third resistance is the pressure drop along the ribbed pattern of the plate within the cell. The fourth restriction is the exit from the cell, and the fifth resistance is a similar manifold for the exit gases.

The most desirable place to include the high pressure drop would be in the cell exit zone, the fourth resistance mentioned above. Only one ΔP source is required per plate, improving reliability. However, the American Cyanamid electrode will weep electrolyte, and droplets can form within the gas compartments. These droplets could block an individual outlet orifice, causing a pressure drop imbalance on a cell-to-cell basis. Therefore, the pressure drop restriction was included in the inlet to the cell from the inlet manifold.

The 100-sq-in. cells are connected hydraulically as two parallel cells on an individual plate. In other words, there are two gas inlets at adjacent corners and a single, larger gas outlet in the center of the opposite side. This configuration was used for the earlier cell design and found to favor uniform gas distribution over the face of the cell. Similarly, it minimizes the size of manifolds, which otherwise might become unwieldy. However, this configuration requires two inlet orifices to the cell, doubling the chance that nonuniformity in the orifice could exist, with subsequent gas maldistribution.

A review of the principles involved in the hydraulic considerations will be presented in the next subsections. A later subsection on experimental pressure drops and gas distribution will refer to these calculated values. After indicating the design parameters, the specific conformation of the hydraulic resistances will be detailed.

5.2.3.1. Pressure Drop Along the Cell Face

Pressure drop of the gas flow along the face of the cell is difficult to calculate or even estimate because the shape of the gas channels in the operating cell is not known with certainty. Not only can the electrode and matrix extrude into the gas flow channels, but there will certainly be a film of liquid between the peaks of the bipolar plate and the electrode. Both of these phenomena would reduce the size of the gas flow channels. As a first approximation, however, we can assume that the gas flow passages consist of a series of parallel tubes of 0.10 in. diameter.

As the air side of the bipolar plate will have a higher pressure drop, it was used as the basis for calculations. A current density of 100 A/sq ft was assumed at 40% utilization efficiency of the oxygen in the air. On this basis, the lineal velocity of the air (not allowing for increased volume due to water manufacture in the cell) is 1.2 ft/s or the Reynolds Number is 64, well within the laminar region. The pressure drop along the 10 in. of path length, under these conditions and at the cell operating temperature, is 0.032 in. of water. This preliminary calculation indicates that the pressure drop along the face of this cell should be low, even with the water generation.

However, the most questionable part of this calculation is the effective diameter of the valley in the bipolar plate. If this diameter is arbitrarily halved to account for the restricting effects mentioned above, as well as the irregular shape and subsequently higher effective hydraulic radius, the pressure drop increases to about 0.5 in. of water. This pressure drop is still low, although higher than would be desired.

The two examples calculated above are believed to represent extremes of possible pressure drops in the operating cell. The 0.032 in. of water approximates an ideal case of the flow between the bipolar plate and a flat hard surface. The 0.5-in. water pressure drop is based upon an effective diameter which is much smaller than expected, considering the geometry of the problem and the plate-to-matrix pressures expected in the operating cell of the improved design. Therefore, we anticipate pressure drops of about 0.1 or 0.2 in. of water across the face of the cell in the improved design.

In the earlier design, much higher pressure drops were encountered. With that embossing pattern, the best possible effective diameter was on the order of the worst expected in the above case; pressure drops of at least 0.5 in. of water would be expected. Moreover, because of high plate-to-matrix pressures, significant extrusion of the matrix into the channels might be expected and flattening of the bipolar plates was possible. This could account for the high pressure drops experienced in the earlier tests.

5.2.3.2. Pressure Drop Through Inlet Orifices

As explained earlier, each cell had two inlets for each reacting gas. The higher pressure drop along the face of the cell was on the air side, so the air orifices were the first to be designed. The inlet orifices are to be the controlling pressure drop within the cell. The orifice pressure drop was taken as 5 times the maximum ΔP expected across the face of the cell or approximately 10 times the pressure drop that might reasonably be expected in operation. Therefore, a pressure drop of 2.5 in. of water was selected for the impedance of the inlet air orifices at the operating conditions. Under the design air flow conditions of 100 A/sq ft with 40% utilization of the oxygen in the air, this pressure drop corresponds to an air velocity of 74 ft/s or an orifice opening of 1.8×10^{-3} sq in. in each inlet. This corresponds to a rectangular hole that is 0.018 in. x 0.100 in. wide. The details of the construction of this hole will be presented in subsection 5.2.3.4.

The inlet orifice for the fuel flow is not designed on pressure drop. Rather, as will be shown in a later section, the gas distribution across the face of the cell is dictated by the velocity of the gas in the inlet orifice. In the interest of uniformity, the compartment frames for both the fuel and air sides were manufactured identically, and the inlet orifices were designed for the same lineal velocity. The velocity in the air orifices was 74 ft/s; consequently the fuel orifice was also specified for this value. At similar fuel consumption, this resulted in an orifice that was 0.018 in. x 0.062 in. wide. The expected pressure drop for the fuel flow through this orifice is about 1.5 in. of water, well above the pressure drop expected for the fuel flow over the bipolar plate.

5.2.3.3. Other Pressure Drops

The other pressure drops in the system must be kept relatively low. The area of the inlet manifold was sized by the rule-of-thumb that the cross-sectional area of a plenum should be 10 times that of the sum of its outlets if all outlets are to have similar flow. With 15 cells in the stack and each cell with a 1.8×10^{-3} sq in. inlet orifice, the total area of the manifold should be greater than 0.27 sq in. This would have required a round hole about 5/8 in. diameter — too large to conveniently fit within the 1-in. cell frame and still permit room for gasketing. Rather, an oblong slot of 3/8 in. width was used. This slot was 3/8 in. wide by 1/2 in. long between the centers of the semicircular ends. The area of this slot was 0.3 sq in. and was sufficiently large to satisfy the plenum-to-orifice relationship.

The manifold for the gas outlet was designed the same as the inlet manifolds. Although this manifold carried double the flow rate of the inlets,* the manifolds were not sized on pressure drops and the manifold was adequate to carry the flow.

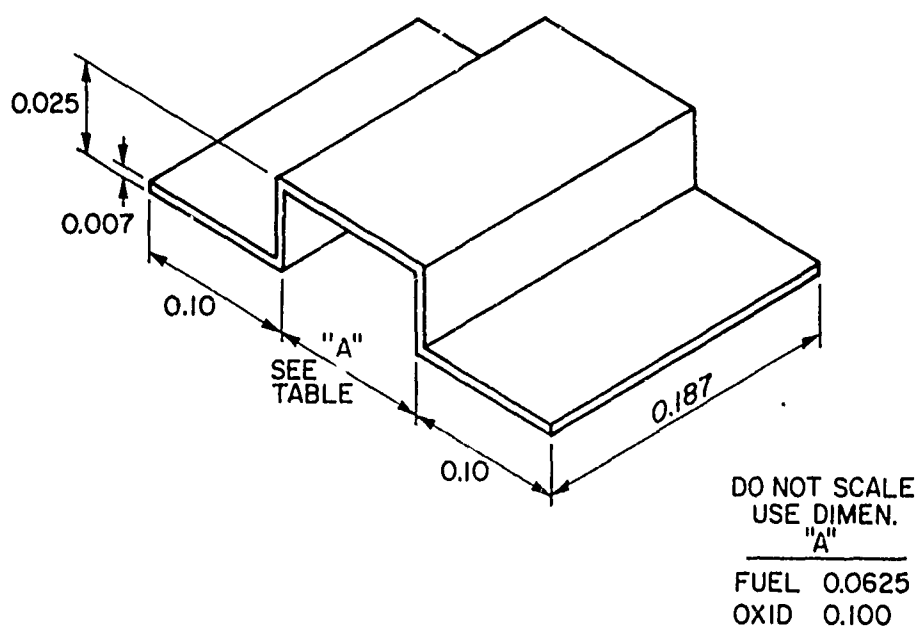
The outlet from the cell to the exit manifold was designed with a factor of 2-1/2 in its cross-sectional area compared with the total of the inlet orifices. Therefore the velocity of the outlet was only 40% of that in the inlet, and the pressure drop was only 16% of the inlet, or 0.4 in. of water.

The total pressure drop across the cell, from inlet manifold to outlet manifold, was less than 3.5 in. of water. Of this pressure drop, 2.5 in. was in the closely controlled inlet orifices, and much of the remainder was in the controlled outlet orifice. Therefore, the cell-to-cell gas distribution should be satisfactory based upon calculated hydraulics.

* There was only one outlet with two inlets.

5.2.3.4. Physical Design of Bipolar Plate Hydraulic Components

The reactant gas inlet orifices were square holes formed by the bipolar plate and a bridge of tantalum, which is illustrated isometrically in Figure 5.5.



A-32260

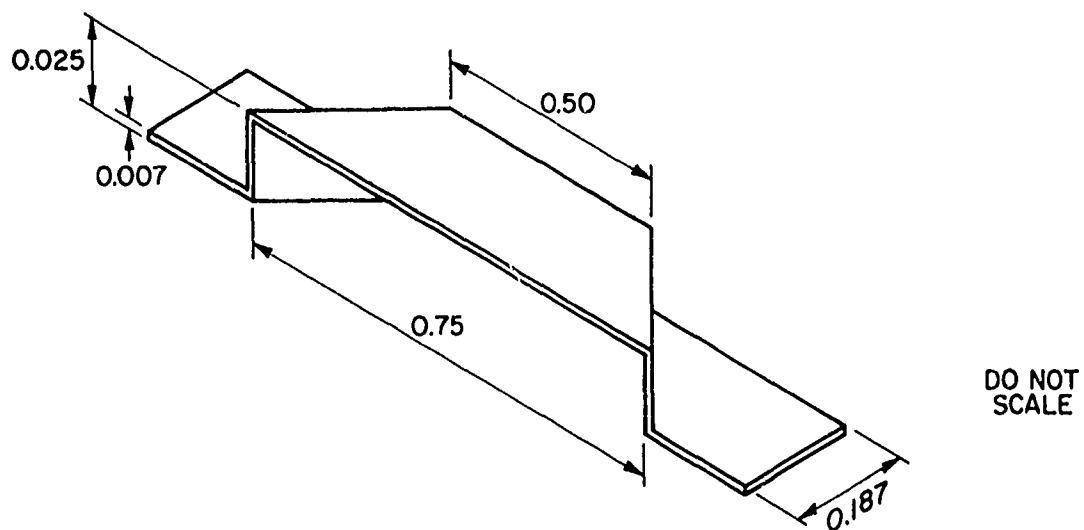
Figure 5.5. ISOMETRIC SKETCH OF INLET ORIFICES

The dimensions in this figure represent the air inlet bridge; the only difference from the fuel inlet bridge is the width of the slot. Significant effort went into the shape of this bridge; this effort will be discussed in detail in subsection 5.3.2. The result of that work was a straight rectangular duct which was 3/16 in. long extending from the inlet gas manifold into the cell compartment plenum. Note that this inlet shape, with its relatively high l/d ratio, probably has a higher pressure drop than predicted by the orifice equation used in the calculations of subsection 5.2.3.2. This higher pressure drop would not be excessive, but would help ensure the uniformity of gas distribution from cell to cell.

The bridges were formed by drawing 0.007-in.-thick tantalum sheet into a die which was 0.025 in. deep and 0.114 in. wide. Then the flanges of the bridge were folded down in a secondary operation. The tantalum bridge formed in this manner has excellent strength for resistance to deformation and constriction of the orifice. These bridges were then spot-welded to the tantalum sheet at precise locations which will be discussed in Subsection 5.3.

The gas outlets from the cell were constructed similarly to the inlet, but with the shape presented isometrically in Figure 5.6. These larger outlets did not have sufficient strength to resist deformation, and auxiliary support, similar to the inlet bridges, were used to brace the center of these outlets.

The slots for the reactant inlet and outlet manifolds were punched in the preformed tantalum sheets with hardened dies. As each gas had two inlets and one outlet, a total of six reactant manifolds were used. In addition, longer slots were cut for internal coolant passages, as will be discussed later. The resulting bipolar plates, with embossed pattern, slots, and welded orifices, are illustrated photographically in Figure 5.4.



A-32261

Figure 5.6. ISOMETRIC SKETCH OF GAS OUTLET

5.3. Gas Compartment Frames

5.3.1. Earlier Design

The earlier 100-sq-in. cells had used gas compartment frames which were hand cut from 0.031-in.-thick ethylene-propylene-terpolymer rubber of 70 durometer hardness. These rubber compartment frames also served as the gasketing material between the columbium bipolar plates and the plastic-impregnated matrix. The frames were 12 in. square on the outside with a 10-in.-sq hole in the center containing the anode or cathode gas. Gas inlets were triangular slots cut to the circular gas manifolds and protected from closing by columbium tabs which were placed over the slot on the matrix side. The triangular shape of these slots helps distribute the gas over the face of the cell.

These compartment frames also serve the purpose of gasketing. The softness of the rubber required for gasketing was probably a detriment in the design of the frame. The soft rubber would possibly compress in the area of the gas inlets, thus causing cell-to-cell gas maldistribution. The preformed orifice, discussed in the preceding subsection, was the design which was chosen for uniform gas distribution among the cells. In addition, the end functions of the materials were separated in the newer design, and the compartment frames were not required to be the gasketing materials. Rather, a harder plastic could be used for the compartment frame, avoiding deformation under pressure because the gasketing would be a separate material.

The shape of the inlet orifice would be determined by the requirements of even gas flow across the face of the cell. Also, pressure-drop measurements were made in this phase of the design.

5.3.2. Materials of Construction

Teflon was chosen as the design material for the compartment frames in this prototype stack because of its inertness and ready availability. In production units, a harder EPT rubber might be chosen on a cost basis. The primary difficulty with Teflon is its tendency to cold-flow. However, the Teflon is not being used as a gasketing material; its only purpose is to provide a shape for the compartment. The Teflon is not under pressure except in those areas where it supports the gasket

(Subsection 5.4). Therefore, any cold-flow would be limited to the area where the Teflon was under force and where the areas were not critical.

The commercially available thicknesses of Teflon are limited, but the number of available thicknesses is much greater than was available for the EPT rubber. Direct calculation would indicate that a thickness of 0.29 in. would be desirable; however, these calculations had proved unreliable with EPT rubber in the earlier cells. Consequently, a number of thicknesses were tried. The first test involved a Lucite holder for a bipolar plate pressed of brass with preliminary gas inlet and outlet ports included. This brass and Lucite apparatus was used extensively in the flow distribution and pressure-drops tests to be discussed later. For these tests, gas compartment frames of various thicknesses were cut and installed with the brass bipolar plate in the clear plastic holder. Then water was introduced to fill the "electrode compartment" and was blown out with low-pressure air. The retained water, at the peaks of the bipolar plates, was examined as a function of compartment frame thickness. This was an indication of the effective contact of the cell. This test indicated that thicknesses of 0.020, 0.025, and 0.030 in. might be satisfactory. Greater thicknesses did not show good plate-to-plastic contact, and thinner compartment frames exhibited bowing with distortion of bipolar plate at the edges and poor contact at the center. Of the three thicknesses considered, the 0.030 in. was marginal, but was included in the following tests because of the possibility of the extrusion and improved contact.

A small, 1/4-sq-ft cell area cell stack was constructed with columbium bipolar plates that had been pressed between polyurethane and a die which was grooved in one direction with the sinusoidal cutter (Figure 5.1, Subsection 5.2.2). This stack was operated with compartment frame gaskets of 0.020, 0.025, and 0.030 in. thick. The thickest compartment frame gaskets resulted in a higher internal resistance in the cell, and the thinnest sheets resulted in stacks or individual cells with lower performance, perhaps because of improper gas distribution. Therefore, the thickness of 0.025 in. was chosen for the new design.

The thickness of the compartment frame gaskets was used to determine the height of the gas inlet orifices, and the design value of 0.025 in. was fed back into the orifice design which was discussed in Subsection 5.2.3.

5.3.3. Flow Distribution

The Lucite holder and the brass bipolar plate were used for empirical gas flow distribution studies. By this time, the open area of the inlet orifice had been determined in addition to the tentative location for the inlet gas manifold: at the sides of the cell near the corners. The gas distribution tests were run to determine the shape of the orifice so that the gas would be distributed evenly across the face of the cell. Throughout the earlier work, even back to the IEM stack, the problem of gas distribution had been attacked by spreading the gas flow as it left the orifice so that it distributed evenly. The same approach was used in this work.

The first tests were run by painting the bipolar plate black and drawing smoke from an oiled cigar to the plastic rig by a water ejector pump. This was a qualitative test which could have been quantified by taking motion pictures of this flow pattern; however, a less expensive quantitative test involved impregnating the matrix with lead or cadmium salts and passing a known quantity of H_2S in the gas stream. The colored area formed on the matrix is a quantitative measure of the velocity of the gas in each area. Still later tests substituted unexposed blue-line Ozalid paper for the matrix, and the inlet gas was passed through an NH_4OH solution.

Many tests were run with varying locations and shapes for the inlet orifice, trying to distribute the incoming gas evenly. However, the results were not satisfactory. The center and edges of the cell continued to get high flow rates, and the other portions were low. The best results gave flows in the high rate sections that were still 3 times those in the lower rate sections. The final design was found by using the velocity head rather than fighting it. All of the earlier work attempted to disperse the gas uniformly; rather, we found it was better to use the gas velocity and bounce it off a properly contoured edge of the compartment. In the final design, the gas was aimed across the cell at the leading edge

of the sinusoidal ridges. The area for flow in this direction was constricted by the decreasing distance between the compartment frame and the ridges. A parabolic shape was chosen as the most desirable with 0.10-in. clearance at the center of the cell, expanding to 0.35 at the edge of the cell.

Figure 5.7 is the drawing of the compartment frame as designed and constructed, and Figure 5.8 is a photograph of the compartment frame. The parabolic shape of the one inside wall is obvious. Also included are the gas inlet and outlet manifold holes and holes for manifolding the coolant liquid (to be discussed in Subsection 5.7.2). A series of grooves are indicated on this drawing, and they will be discussed in the next major subsection (5.4) under Cell Gasketing.

The parabolic design for one edge of the compartment frame indicated that a simple, straight orifice could be used, rather than the complicated-shaped orifices which had originally been considered. Therefore, the design of the inlet orifices was fixed as presented in Subsection 5.2.3.

5.3.4. Pressure Drops

The Lucite holder and brass bipolar plate assembly was used for determining the pressure drop across a mock-up of an individual cell. Pressure taps were drilled in the inlet manifold at two locations along the inlet side of the cell and at two places along the outlet edge of the cell. Pressure-drop measurements were made with an inclined manometer having a readability of 0.01 in. wc. The pressure drops for air flow are presented in Table 5.1 in terms of inches water column as a function of air-flow rates to the cell. For comparison purposes, the air flow required at 100 A/sq ft and 40% utilization of the oxygen is 26.3 standard cu cm of air per second through one-half of the cell.

The data in Table 5.1 will illustrate that the pressure drop across the face of the cell is so low as to be nonreproducible. In fact, many values are negative in regions where the flow or dye tests proved a proper direction of flow. The indicated pressure drop to the inlet orifice is significantly lower than calculated — at most 10% of the estimated ΔP . However, this test rig was not gasketed as well as the operating cell's

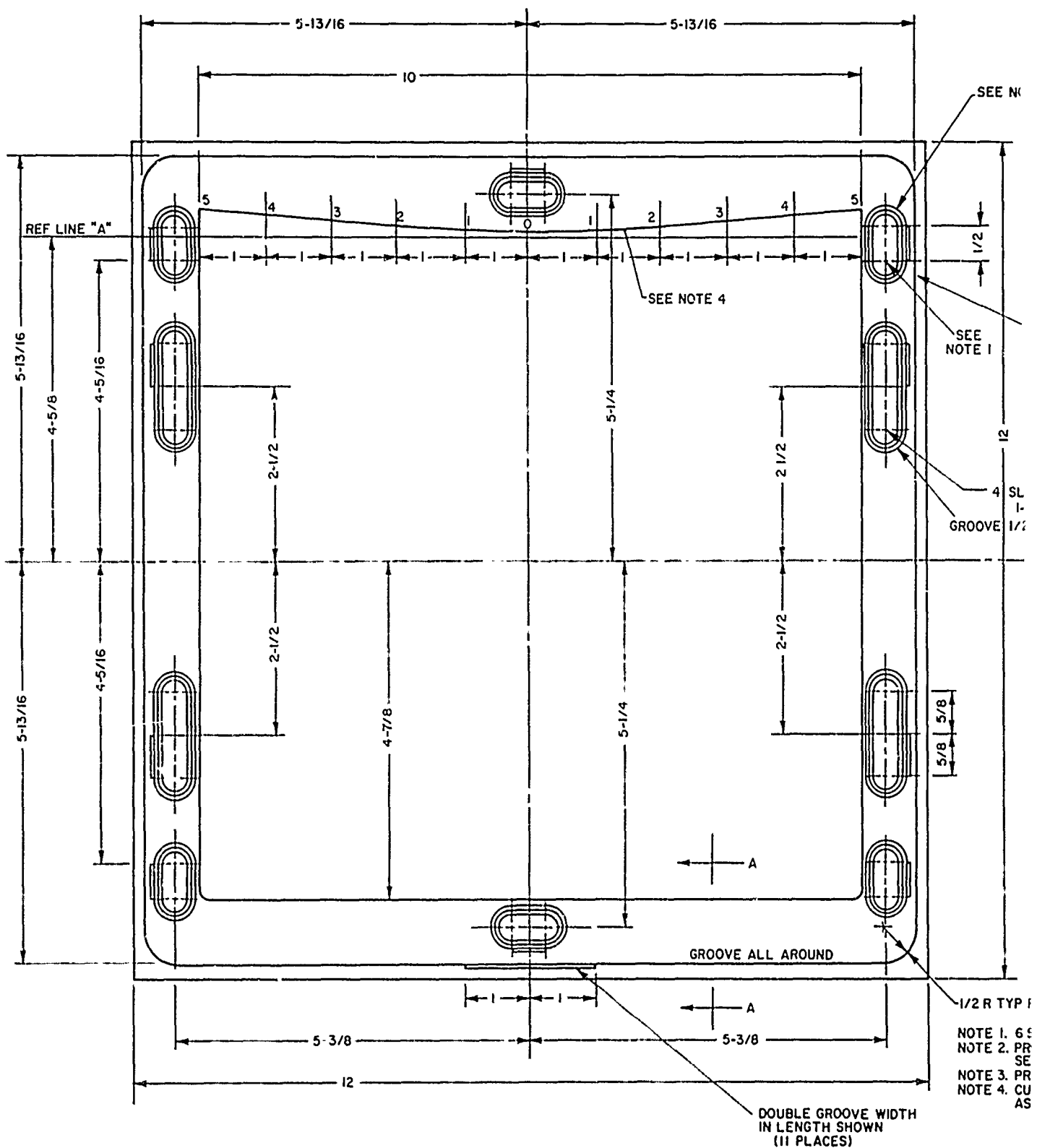
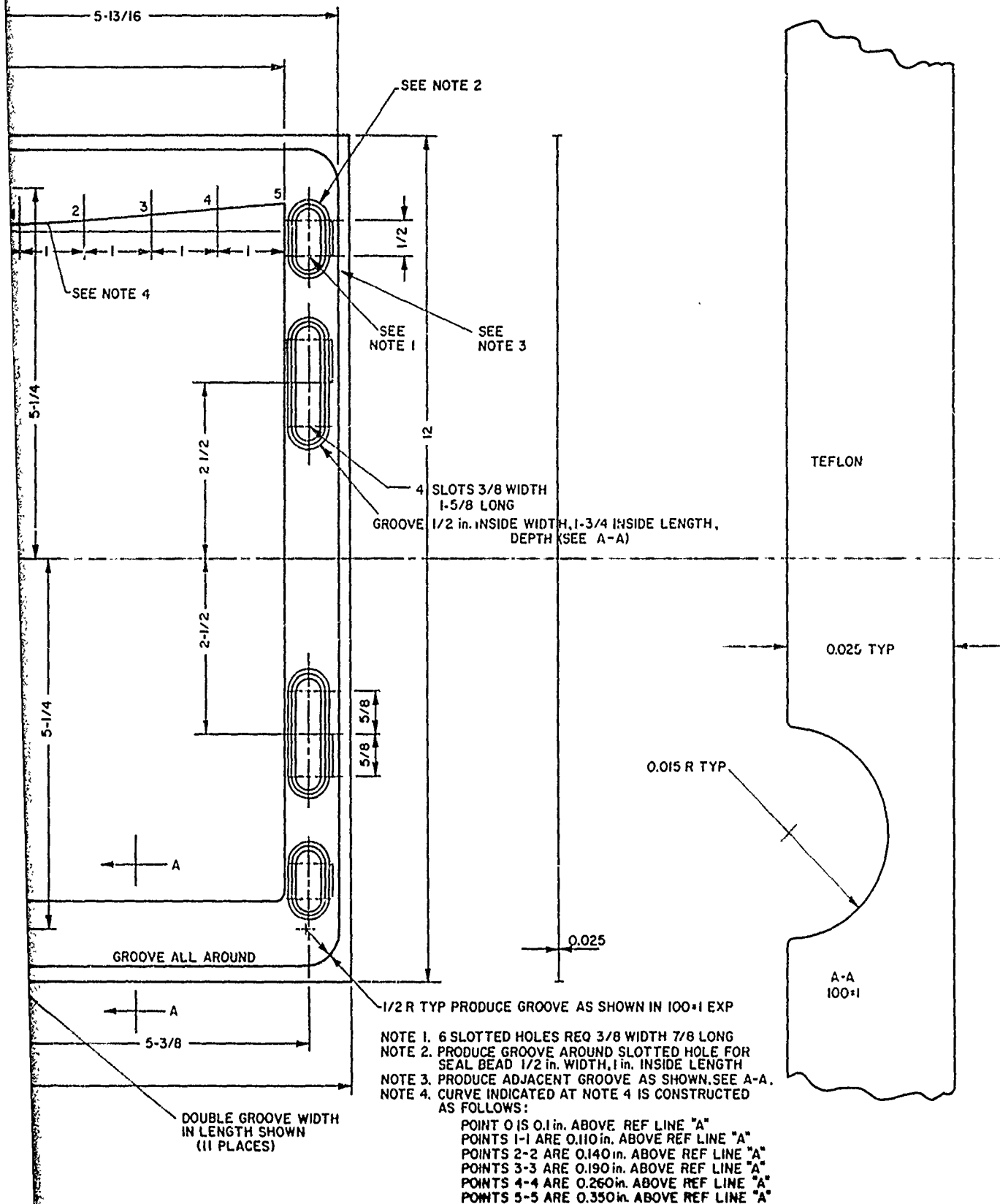


Figure 5.7. ENGINEERING DRAWING OF COMPAR

B



D-32272

ENGINEERING DRAWING OF COMPARTMENT FRAME

Reproduced from
best available copy.

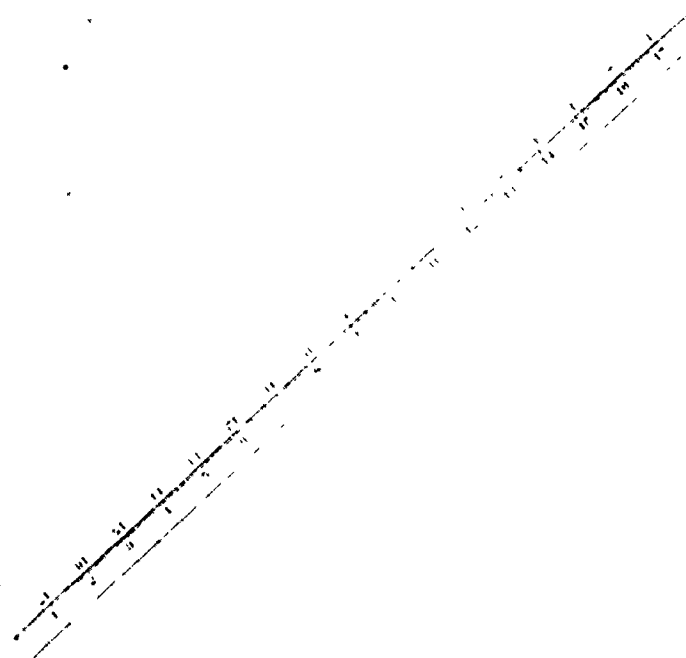
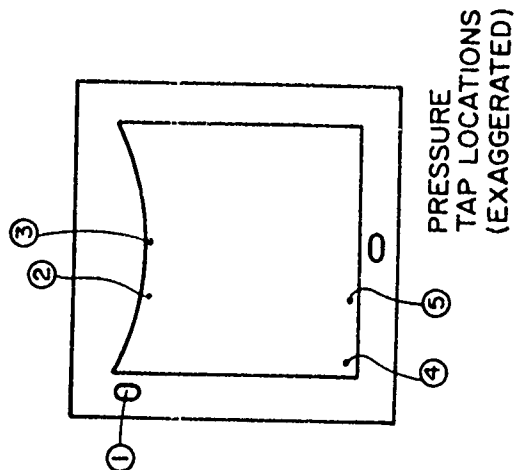


Figure 5.8. PHOTOGRAPH OF TEFLON COMPARTMENT
FRAME (Air Compartment)

Table 5.1. PRESSURE DROPS FOR AIR FLOW

Tap Location	Normalized ΔP to Exit				
	Flow Rate, cu cm/s				
	25	50	60	75	100
	in. wc				
1	0.33	0.74	1.24	1.64	3.36
2	0.14	0.40	0.67	0.82	1.36
3	0.12	0.41	0.56	0.71	1.41
4	0.15	0.44	0.68	0.83	1.61
5	0.12	0.43	0.60	0.86	1.62
	Other Normalized ΔP 's				
	Flow Rate, cu cm/s				
	25	50	60	75	100
	in. wc				
Inlet	0.19	0.34	0.57	0.82	2.0
1-2 (orifice drop)					
Cell Face					
2-4	-0.01	-0.04	-0.01	-0.01	-0.25
3-4	-0.03	-0.03	-0.12	-0.12	-0.20
2-5	+0.02	-0.03	+0.07	-0.04	-0.26
3-5	0.00	-0.02	-0.04	-0.15	-0.21



A-32269

in the stack, and some leakage around the orifice might have been possible. Also, the measured inlet pressure drop is an order of magnitude larger than the apparent pressure drop across the face of the cell, indicating that satisfactory cell-to-cell gas distribution will be accomplished and controlled by the orifices. However, the outlet pressure drop was relatively high. These tests had used a matrix so as to simulate possible extrusion into the gas channels, and this matrix may have caused flattening of the bridge in the original design of the gas outlet. Consequently, the gas outlets were reinforced in the later designs.

5.4. Cell Gasketing

As explained in Subsection 5.3.1, the initial design used a combination of gasket and compartment frame. The entire area of the compartment frame was used to seal the cell. The philosophy in this design was to separate the functions of compartment frame and gasketing. The large area of sealing was to be avoided, and line-sealing similar to O-rings was to be used.

The first approach was to consider molding the Teflon compartment frames with a ridge in the area where gasketing was desirable. However, the time, cost, and reliability of this molding was undesirable. This philosophy might still be used in a production unit, but a less expensive expedient was used in this prototype.

The compartment frames were punched out of sheets of Teflon. The same die incorporated a series of ridges which would form grooves in the gasket area of the compartment frame. These grooves were etched, and rubber cord was glued in place for the gasketing.

The finest diameter of EPT rubber cord which was obtainable was 1/32 in., although 0.020 in. would have been desirable for this application. Grooves around all the manifolds and around the exterior edge of the cell were formed in the Teflon with a 0.015-in. radius. Thus, all six of the gas manifolds and the four coolant manifolds were individually sealed. Another seal was used around the cell periphery. Individual O-rings were not used, rather the cord was glued in place and overlapped. This discussion explains the series of grooves in the drawing of Figure 5.7.

The area of the grooves in the Teflon was etched with proprietary product produced by Chemplast, Inc. This permitted adhesion of the glue. The peroxide-cured 60 durometer EPT rubber cord was glued in place with EPT rubber cement and air dried. The gasket-frame combination was mounted in a jig with a bipolar plate, and the rubber cement was cured at 150°F for 2 hours. This procedure was tedious and time-consuming; however, the results were satisfactory. Not only was the frame gasketed and sealed to the bipolar plate, but an improved seal was made with the Kel-F impregnated matrix on the other side of the Teflon.

5.5. Electrodes

One basic premise for this program was the commercial availability of the American Cyanamid electrodes. American Cyanamid had developed the technology for the manufacture of uniformly active electrodes. These electrodes became generally available in 1964 and spurred much of the fuel cell research in this country. A second major advance by American Cyanamid was the development and commercial availability of the CO-tolerant anode catalysts. These anodes permitted fuel cell operation with up to 3% carbon monoxide in the fuel, as evidenced by the earlier IGT work under this contract, and indicated promised for direct hydrocarbon fuel cells.

The program Sponsor, USAMERDC, opted to develop fuel cell hardware under this contract, with American Cyanamid continuing basic electrode development work. However, midway through this program, American Cyanamid discontinued the production of commercial electrodes. Without a supplier of commercial electrodes, this effort was terminated when the available stock of electrodes was exhausted.

5.5.1. Cathodes

The cathodes used in this stack development program were the American Cyanamid Type AA-3 electrodes containing 5 milligrams of platinum per sq cm of electrode area. The electrode support material was expanded tantalum sheet. These electrodes had proved satisfactory as air catalysts in low-temperature phosphoric cells in earlier work under this contract. They were expected to operate even better at the slightly higher temperatures to be used with the new stack design.

5.5.2. Anodes

The anode catalysts used in this fuel cell stack development program were American Cyanamid Type RA-2 electrodes containing 5 milligrams noble metal per sq cm. The noble metal was 50% platinum and 50% rhodium. An additional synergistic material added to these catalysts by American Cyanamid was an amorphous tungsten oxide, which enhanced the resistance of these catalysts to carbon monoxide poisoning. Electrodes of this type had operated satisfactorily with up to 3% carbon monoxide in the feed in our earlier work. They should also operate satisfactorily at the higher temperatures expected in this program.

We had considered using anodes of the RA Type containing only 2 milligrams per sq cm of noble metals. However, this program was directed at improvement of stack operating hardware, not electrode assessment. Although we believe that the lower loading electrodes would have operated satisfactorily in the temperature range of 250⁰-275⁰F with 3% carbon monoxide in the fuel, they were not used because their performance was not a certainty.

5.5.3. Alternative Electrode Sources

With the discontinuance of the American Cyanamid electrodes, completion of this hardware development program became just a design exercise. However, should other electrodes become available, this design may again offer value as a prototype.

A desirable electrode for the cell design should, of course, have high catalytic activity in the hydrogen-oxygen system. Also, the anodes should have resistance to carbon monoxide poisoning to minimize the fuel pretreatment requirements. Another desirable attribute would be a conductive, hydrophobic film on the gas side of the electrode. This film would conduct electricity from the catalyst site to the bipolar plate, yet would eliminate the electrolyte weepage that occurred with the Cyanamid electrode. With this electrode modification, the stack could be constructed with high-grade stainless steel bipolar plate. These plates would be significantly less expensive than the tantalum plate, yet could be satisfactorily gold-plated for minimum contact resistance.

5.6. Matrices

Previous work under this contract had been done with electrolyte-containment matrices made from fibrous glass filter paper. We had experienced significant degradation problems with time and/or temperature because of the corrosive action of the phosphoric acid upon the glass. Before the inception of this design program, additional matrix materials became available which were capable of operating at higher temperatures. One purpose of this program was to evaluate these newer matrix materials.

The matrices were cut to the full size of the bipolar plate, and the inactive gasketing area of the matrix was blinded by impregnation with a solution of Kel-F 800 in methyl-ethyl-ketone. When the ketone had evaporated, an effective edge seal was formed in the matrix. In essence, this patented process permits the matrix to become its own gasket. Then, holes were punched in the matrix for various gas manifold holes.

In general, the design of the matrix had proved satisfactory in the past. Therefore, the same edge sealing-gasketing technique would be used in the new stack design. The primary difference was the inclusion of punched holes for recirculating coolant manifolds in addition to the holes for the gas manifolds. When the program was changed to air-cooling of the stack, these holes were not punched in the matrices although they were still open in the bipolar plate gas frames.

5.6.1. American Cyanamid Teflon Matrices

American Cyanamid Co. developed a matrix material that appeared to be made of etched Teflon felt. The matrix was inert to acid attack, as is characteristic of Teflon, but had been etched to a deep brown color so that it was no longer hydrophobic. The initial material delivered from Cyanamid was presoaked with water so acid impregnation was not a problem. The water in the matrix was simply replaced with acid by successive washings. However, the water-soaked matrix was not amenable to the IGT edge-gasketing process. Subsequently, American Cyanamid developed a dry matrix that could be post-wet with electrolyte before assembly. This matrix was suited to the Kel-F impregnation technique.

The following difficulties were found with the American Cyanamid Teflon matrix:

1. This matrix construction was dimensionally unstable. The matrix grows or shrinks, apparently at random, after it has been rewet. This problem was partially alleviated by the Kel-F edging, but aligning the holes of the matrix with those of the rest of the stack was difficult and required stretching of the matrix. This stretching of the matrix probably weakened its structure and physical resistance to gas crossover. Moreover, any slippage during stack assembly and compression would result in misalignment of the manifold holes and possible cross-flow of reactant gases.
2. The electrolyte could not be satisfactorily recharged to a stack in normal maintenance. The American Cyanamid electrodes will weep a slight quantity of electrolyte, requiring periodic refilling of the matrices with fresh electrolyte as a normal maintenance procedure. However, perhaps because of the techniques required to wet the matrices, these electrodes could not be satisfactorily recharged.
3. The matrices became hydrophobic with time. The etched surface of the Teflon was removed with time, particularly at the cathode side of the matrix, and the matrices became white and hydrophobic. Under these conditions no acid could be recharged, and gas crossover was possible.

Although this matrix is satisfactory for operation in the short term, it was not selected for the stack operation due to the availability of other materials.

5.6.2. Union Carbide Tantalum Oxide Matrix

Union Carbide Corporation developed a matrix material that appeared to be a replica of a woven cloth. Based on its appearance, this material had possibly been made by impregnating a cloth with solution of a tantalum salt and then burning off the cloth leaving tantalum oxide. The resulting fabric-like material was inert to attack by the phosphoric acid electrolyte at the operating temperature of the stack and appeared to have reasonable bubble pressure for resisting gas crossover. However, the material was extremely fragile. Microscopic cracks, which could decrease the bubble pressure rating, would form during handling in either the dry or wet state. In particular, the matrix would crack along the edge of the Kel-F treated zone. Because it was so fragile, this matrix material would not be satisfactorily employed alone in this stack construction. However, it could be used in combination with stronger materials such as that described in the following subsection.

5.6.3. Pratt & Whitney Matrix

The Pratt & Whitney Aircraft Division of United Aircraft Corporation had developed a proprietary matrix under the TARGET program for use in its acid fuel cells. This matrix was several steps superior to the commercially available matrices in wet strength and bubble pressure. It was somewhat fragile when dry, but did not exhibit the extreme breaking tendencies of the tantalum oxide matrix. However, when the edges were impregnated and the active area was wetted with electrolyte, this matrix became quite strong and handleable. Nevertheless, a double matrix was desirable for reliability. This was the primary matrix chosen for use in the stack development work.

5.6.4. Matrices Used During Tests

After preliminary tests of the individual matrix materials, the primary matrix selected from the three candidates was that manufactured by Pratt & Whitney. However, the Pratt & Whitney TARGET program had since progressed to a still better matrix material, and the supply of the matrices described in Subsection 5.6.3 was limited. There was insufficient matrix material available to use double-thickness matrices in all cells of the test battery. Consequently, some cells use a single thickness of the Pratt & Whitney matrix with a single thickness of the Union Carbide matrix for a combination of sufficient electrolyte reservoir with reliable wet strength. In general, those cells selected for the mixed materials were the center cells of the three cell modules between cooling plates. These cells would have less stress placed upon the matrix at the edge of the gas compartment because of the greater compressibility of material between that cell and the hard coolant plates. In addition, the internal edges of the gas compartments in those cells were carefully sanded smooth to avoid cutting the matrix.

5.7. Coolant Plates

The coolant plates used in the original IGT battery stack design were integral with the end plates. Under the design principle of separation of function, the coolant plates were a separate component in this program.

Two types of coolant plates were designed under this program. After the original liquid coolant plates had been designed, a contract modification was written to use air coolant, which would be more satisfactory to both IGT and the Sponsor.

5.7.1. Previous Design

The combination coolant-end plates of the previous design were constructed from 1/2-inch stainless steel plate. The 10-in.-square center area of the plate was hollowed out for coolant flow. The coolant entered one side of the plate through a 1/4-inch stainless tube and made multiple passes before exiting the plate through a similar tube. The multiple passes were generated by 3/8-inch-high dividers within the open area. The faces of the coolant section were 1/16-in.-thick stainless sheets which were continuously welded to the original 1/2-in. plate in a relief area. The 3/8-in.-square dividers were spot-welded to the bottom face plate, and the top face plate was installed and continuously welded around the edges. The entire assembly was again spot-welded to the dividers. Then the assembly was surface-ground for flatness.

The combination end plate-coolant plate had problems in both functions. The difficulty experienced in the end plate use are discussed in Subsection 5.8. The primary problem with the use as a coolant plate was the high internal pressure drop for the coolant flow required. The spot-welded assembly with the thin face plates had insufficient strength to withstand the high internal pressures generated within the coolant plate because of the small size of the inlet and outlet passages. Consequently, the spot-welds would fail, and the thin facing would bulge under the internal pressure. This bulging caused improper loading upon the cell stack, with insufficient force in the sealing area, but excessive loading in the active area of the cell. Less serious faults experienced in the previous design were the excessive weight and thickness of the coolant plates.

5.7.2. Liquid Coolant Plates

Hollow plates were to be designed for circulating liquid coolant within the cell stack. Preliminary design estimates had indicated that coolant plates should be inserted at least every five cells for uniformity of temperature from cell to cell within the stack. A refined calculation predicted a more desirable coolant spacing of every three cells based upon temperature variations, overall stack dimensions, and other considerations.

These bipolar plates should be thin and lightweight, yet they must be strong enough to resist the compressive forces within the assembled stack. The plates should be electrically conductive, as they will be operated bipolarly, and should be thermally conductive for uniform temperature distribution within the cell stack. However, they must be corrosion-resistant to avoid the attack of the concentrated phosphoric acid electrolyte under electrical potential.

We decided to make the coolant plates out of solid copper with tantalum sheathing. The copper sections of the plate would be made of several pieces which would be soldered together with metallic tin. The melting point of tin is high enough to avoid problems during normal stack operation, yet low enough to avoid annealing the copper or oxidation of the copper during the soldering. Copper was used in the prototype design because of its ease of handling; in a production unit, aluminum would probably be substituted for weight savings.

The coolant plate was designed to the full size of the bipolar plates. It used a 1-inch-wide solid frame around the coolant area, and this frame contained the holes for the various gas and liquid manifolds. The frame was chosen as 1/8 in. thick as recommended by the calculations in the next subsection. The faces of the coolant plates, before the tantalum sheathing, were made of 0.020-in. dead-soft copper sheet which was pressed to the wave and ridge configuration of the bipolar plate. Reinforcing strips of 1/8 in. by 1/4 in. were included between the two faces of the copper plate for carrying the compressive loads.

5.7.2.1. Liquid Coolant Plates - Hydraulic Design

If the coolant plates are located every three cells, the heat load per plate is 539 Btu/hr at 100 A/sq ft if the operating voltages are 0.50 V. At 3°F temperature rise across the plate, the liquid flow requirement is 180 lb/hr if water is used for the coolant; up to double this flow rate is required for some oils. Based upon water coolant, the lineal velocity of the water in a single pass across the plate is 0.13 ft/s for a 1/8-in.-thick plate. This flow rate is low, even if oil with lower density and heat capacity is used. Therefore, the coolant plate need not be thicker than 1/8 in. It cannot be much thinner because of the manifolding problems suggested in the next paragraph.

The inlet orifices from the inlet liquid manifold into the coolant compartment were sized for a pressure drop of 1.5 psi. With an orifice coefficient of 0.6, the velocity at these orifices is 9 ft/s. At the required water flow rate, the total area of the orifices should be 0.0128 sq in. The maximum hole size which should be used for an orifice is 1/16 in. to provide sufficient material for around the hole for physical strength. As a 1/16-in.-diameter hole has an area of 0.003 sq in., at least four such holes would be required. In the interest of uniformity of liquid distribution across the coolant plate, two sets of three holes each were used, one set for each half of the plate. This required two liquid inlet manifolds equally spaced from the center line of the coolant flow. The orifices from these manifolds to the coolant chamber used one larger hole of 1/16 in. diameter, which was impinging on one of the reinforcement bars, and two smaller holes of 0.0465 in. diameter (No. 56 drill), which were set at a 45-degree angle to the direction of coolant flow. The total flow area of the six holes is the required 0.0128 sq in.

The size of the orifices leading from the coolant compartment into the exit manifolds should be large to permit a primary flow-regulating device in a single location (the inlet orifices). Each of the two outlet manifolds had five holes of 1/16 in. diameter for a total open area which was 2.5 times that of the inlet orifice.

Manifolds were sized by the rule of 10: that the area of the manifolds should be at least 10 times the area of the total outlet for uniform flow distribution. With six coolant plates on a 15-cell stack, each manifold should be a minimum of 0.382 sq in. in cross-sectional area. We used slots that were 3/8 in. wide by 1-1/4 in. between the centers of the rounded ends to provide sufficient cross-sectional plenum.

The hydraulics of the cell were based upon water flow. With oil flowing at a lower density and lower heat capacity, the pressure drops within the orifice could climb toward 10 psi. Yet, the pressure drop in the exit manifolds and orifices was low so that the internal pressure within the cell coolant plate would not be excessive.

The coolant plate was tested using hot water. The finished plate was chilled with dry ice and exposed to high humidity until a heavy layer of frost had formed. Then, hot water was forced through the cell, and the patterns of melting of the frost were observed. The tests with this hydraulic design in the plate showed a uniform advance of the melting with time, indicating an excellent distribution of the hot water in the inlet manifolds.

5.7.2.2. Liquid Coolant Plates — Mechanical Design

As indicated above, the basic material for the construction of the liquid coolant plates was copper. Half-hard copper bus-bar stock of 1 in. x 1/8 in. x 10 in. or 12 in. long was machined with the gas and coolant manifolds and for the coolant inlet and outlet orifices. These bar stocks were hard-brazed to form a frame which was 12 in. square with a 10-in.-sq coolant opening. The faces for the coolant plate were made from 0.020-in.-thick dead-soft copper sheet which was 12 in. square. These were pressed to the wave pattern of the bipolar plate using the Hydroforming technique followed by the male and female die-set. Then the manifold holes were punched with the same dies that were used for the tantalum bipolar plates. The two faces of the coolant plate were separated by 1/8 in. x 1/4 in. copper strips arranged longitudinal to the direction of oil flow and occupying 30% of the open volume of the frame of the coolant plate.

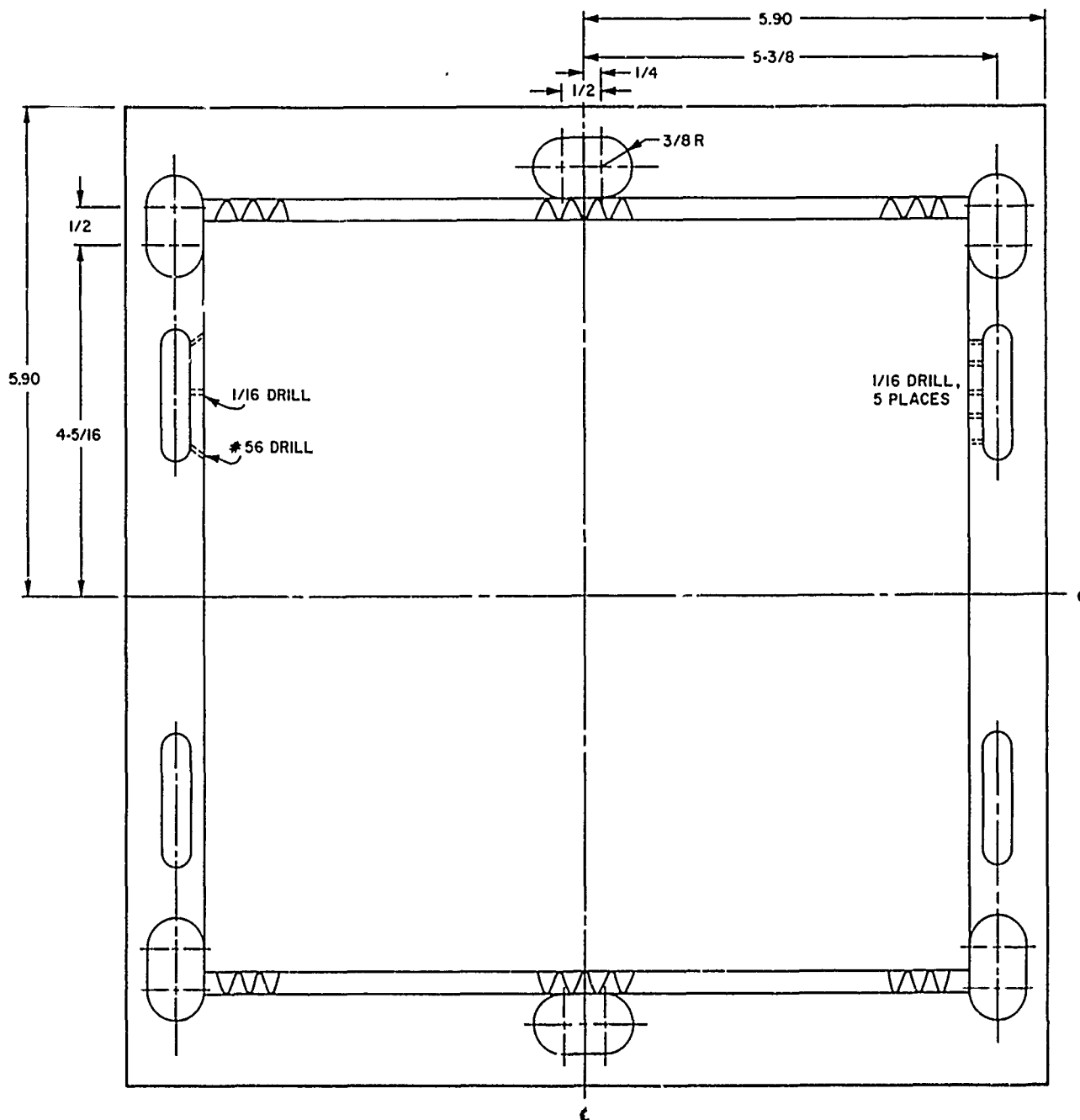
All of the copper parts were cleaned and plated with 0.002-in. tin. They were painted with a solution of rosin in alcohol for flux, and 0.001 in. of tin foil was added between the parts during assembly. Aluminum wires were inserted in all drilled holes. Then the assembly was sweat-soldered between the steel dies (with stainless steel shimstock facing) under 10-ton force for 2 hours at 550°F. The resulting assembly was exceptionally strong and, as indicated in the previous subsection, had excellent flow distribution and heat removal characteristics. Figure 5.9 is an engineering drawing of the liquid coolant plate, and Figure 5.10 is a photograph of a finished plate.

5.7.2.3. Liquid Coolant Plates — Corrosion Protection

The liquid coolant plates were made of copper with a thin layer of tin plating. These would have little resistance to acid attack should it occur. A weak concentration of acid can be expected in the gas outlet ports because of weepage of the American Cyanamid electrodes. A more important consideration is the stronger acid that would be present when the matrices of the cell stack are resoaked in situ. This resoaking step involves introduction of concentrated acid into the anode and cathode gas compartments through the gas inlet or outlet manifolds. A third potential source of corrosive acid in the stack is the wicking action of the matrix during operation. If the edge sealing of the matrix is unsatisfactory or the EPT rubber cord gasketing is imperfect, some acid may leak to the copper through the matrix itself.

Of course, the faces of the copper plate were covered with tantalum sheet. This tantalum sheet was pressed as a bipolar plate and, in this instance, the entire coolant plates became a bipolar unit.

The gas and liquid coolant manifolds should be lined for protection against acid attack. The first design approach was the casting of EPT grommets for this service. The gas manifold grommets were designed for 0.015-in. thicknesses inside the manifold with 0.015 in. x 0.175 in. flanges outside the tantalum sheets. The inside shape of the grommet was oval to correspond with the shape of the manifold. Similar, but longer, grommets were designed for the liquid distribution manifold. However, these longer grommets had slots in the main wall of the grommet to permit flow of liquid into the coolant plate.



D-32260

Figure 5.9. ENGINEERING DRAWING OF LIQUID COOLING PLATE FRAME

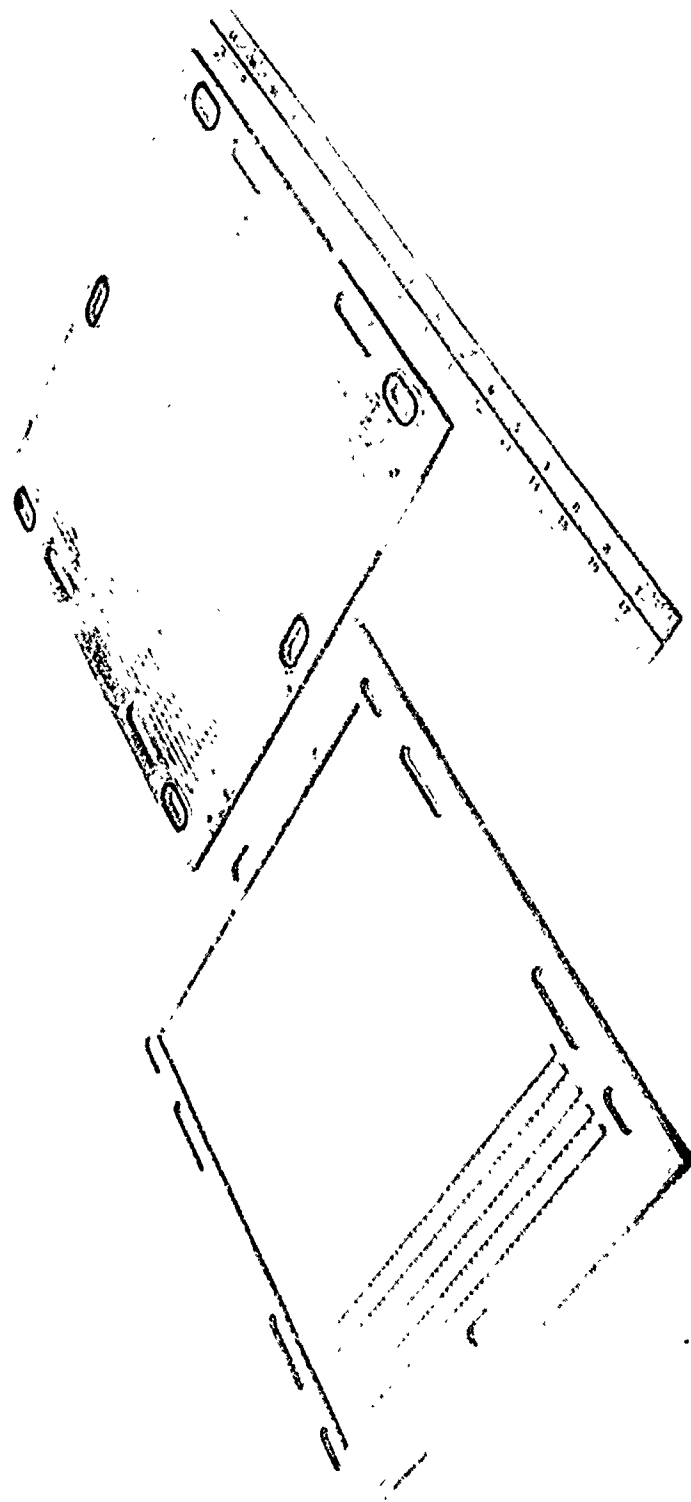


Figure 5.10. PHOTOGRAPH OF PARTIALLY ASSEMBLED
AND COMPLETED LIQUID COOLING PLATE

Despite the assurances to the contrary, our supplier could not satisfactorily mold or dip these grommets of either EPT or Viton rubber, and other suppliers were reluctant to attempt the job. Therefore, we used a back-up design for the sealing of the gas manifolds in the copper plates.

Interts were made for the copper plates out of Kel-F. These inserts (Figure 5.11) were oblong doughnuts with the same thickness as the copper plates and an internal hole the size of the gas manifolds. Grooves were cut in both faces of the insert to accept standard-sized Viton O-rings which sealed against the tantalum cover plate. The gas manifold holes in the copper coolant plates were machined oversized to accept these inserts.

The same technique could not be used with the liquid coolant manifolds because there was insufficient thickness in the coolant plate for two O-ring grooves as well as the coolant orifice holes. In other words, the amount of Kel-F stock between the edge of the larger liquid orifice outlets and the face of an insert was only 0.050 in., insufficient to permit cutting a groove for an O-ring without the possibility of communication to the orifice. Also, if an O-ring groove could be cut, the force of the O-ring would possibly close the liquid inlet orifices. However, the liquid manifolds were not as subject to acid attack. Therefore, simple sheet gaskets were cut of Viton for insertion between the copper plate and the tantalum cover sheet for protection of the face of the copper coolant plate.

5.7.2.4. Liquid Coolant Plates - Operational Difficulties

Difficulty was experienced in both the construction and the operation of the liquid coolant plates. These difficulties caused a delay in the program and necessitated the conversion to air-cooling plates (next subsection) - a contract modification desirable to both IGT and the Sponsor.

One design problem has been discussed above: the specification of the rubber grommet for protection of the gas and liquid manifolds. The second design problem was the thickness of the copper sheets used for the faces. Very poor impressions could be made in sheets of this thickness because of the work-hardening characteristics of copper. The sheets were pressed, annealed, cleaned, and repressed to obtain acceptable

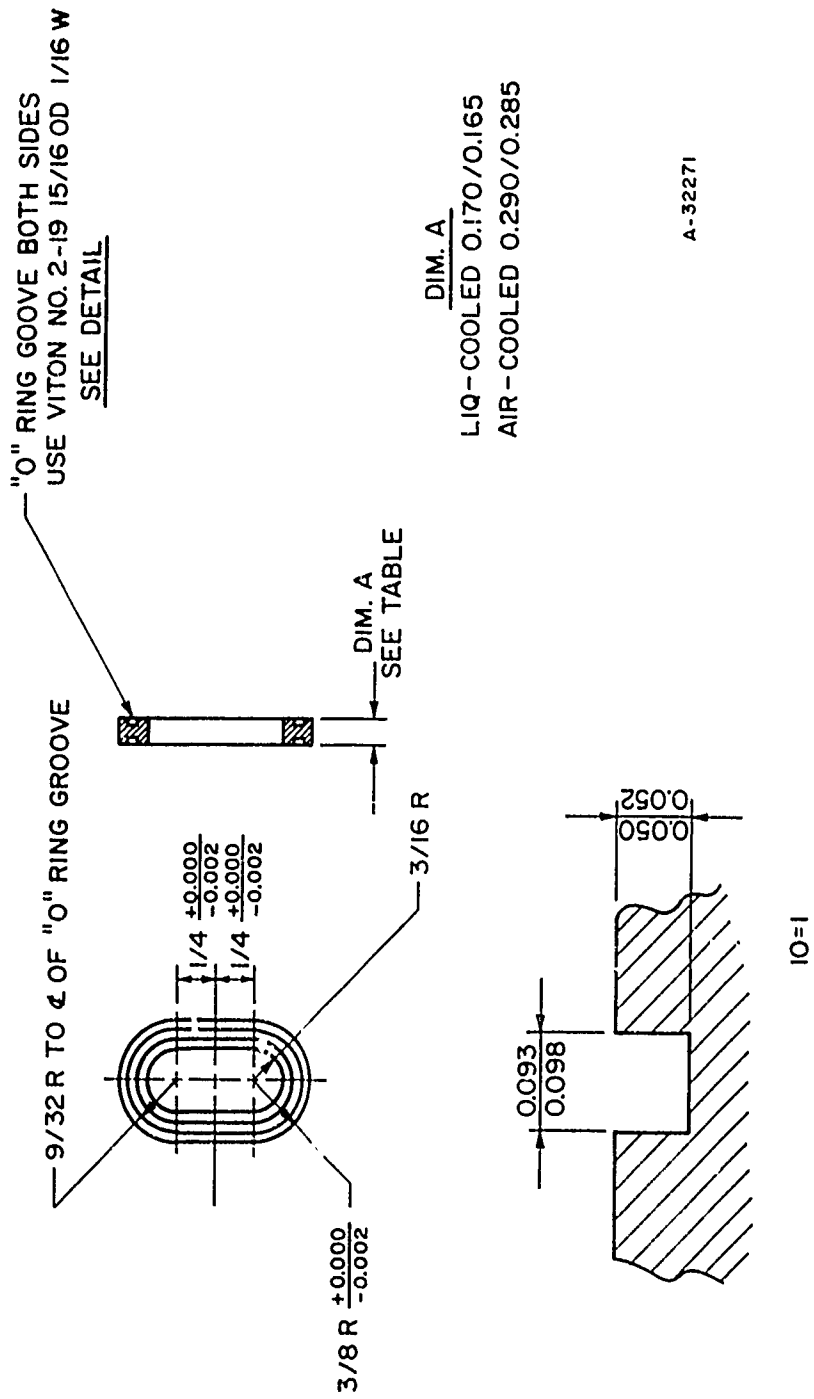


Figure 5.11. ENGINEERING DRAWING OF PLASTIC INSERT FOR COOLANT PLATE

wave pattern definition. Third, the quantity of tin used in the sweat-soldering was excessive, causing blockage of the liquid inlet and outlet holes. In addition, the aluminum wire was not readily removed from these orifices. With practice, however, it was possible to clear these holes by pressurizing the internal chamber of the plate (usually one hole was open) and judiciously heating the hole to be cleared. Too much heat, however, would cause a separation of the face sheets from the frame material.

Operation with the silicone oil coolant was unsatisfactory because we could not satisfactorily contain it with gaskets. Much lower assembly forces were used in the construction of the new design cells compared with the earlier design, but the unit pressures on the gaskets were still high. Yet, the oil would leak in nearly every location: between the end plates and the outside coolant plates, between the coolant plates and the tantalum sheet, between the tantalum and the Teflon compartment frame, and between the Teflon compartment frame and the matrix. Leaks of this nature had not been a problem with the earlier design, perhaps because of the lower temperature of operation or the much higher assembly forces used. Yet any leakage of oil into the gas compartments is a serious electrochemical problem and must be avoided. Postmortem examination of the problem indicated that the oil was significantly wrinkling the EPT and Viton rubber gaskets and that this problem had been avoided earlier because of the mass of rubber utilized.

Consequently, the internal manifolding of the oil coolant was abandoned. The manifold ports in the coolant plates were sealed on the faces by machining a relief section in the original face and soft-soldering a patch on each face. The external manifolds were constructed of 1/4-in. copper tubing which was flattened in the area where it entered the oil port through the edge of the copper plate. The various manifolds were interconnected with Teflon tubing fittings for electrical insulation. This external manifolding arrangement caused high pressure drop and insufficient flow of oil for proper cell cooling. The high pressure drop in the exit manifold caused excessive pressures within the coolant plates. Although the plates were sufficiently strong, the soft-soldered patches on the inlet manifold port exhibited leakage problems. The combination of

high pressure drop, insufficient cooling, and persistent oil leakage forced the termination of the oil coolant program and the redirection of the project toward air cooling of the stack.

5.7.3. Air-Cooling Plates

Midway through the program, the contract was modified to substitute air cooling of the cell for the liquid coolant.

The liquid-cooled cell, discussed in the previous subsection, embodied a bipolar coolant plate included between every three cells in the stack for removing the by-product heat of reaction. This system has the following advantages:

- Low temperature differential across the cell
- Low coolant volume rate
- Low pump power

Perhaps more importantly, its advantages included the possibility of increased system efficiency by boiling water within the coolant plate for feed to the reformer.

By changing to air cooling, we eliminate the coolant pump and recirculating liquid system. If a reformer is not used, the liquid system no longer provides an efficiency incentive and results in only unnecessary weight. Also, the gasketing of the liquid coolant system for internal manifold is difficult, particularly when oil is used for the coolant. With air cooling, both design and physical tolerances appear simpler.

The air-cooling system involves separate cooling and process air. The process air was still internally manifolded to the individual cells, and the flow rate was set for optimum moisture control and voltage of the cells. The coolant gas was independently flow-monitored and temperature-controlled. Separating these functions permits a much wider range of operating conditions for the stack. Further, this type of cooling does not require redesign of any stack structures other than the bipolar coolant plate.

We replaced the existing liquid-cooling plates located every three cells in the stack with plates designed for air cooling. The air-cooling plates weighed about 10% less than the liquid-cooling plates. The aluminum duct work for the air system was much lighter than the coolant pump, storage tank, piping system, and liquid inventory.

5.7.3.1. Air Coolant Plates — Hydraulic and Thermal Considerations

The air coolant plates were first designed empirically, as discussed in the next subsection, at double the thickness of the liquid coolant plates, or 1/4 in. Then, the operating conditions were estimated as follows: If the bipolar air coolant plates are located every three cells and the stack is operated at design conditions, the heat load on each air coolant plate is about 100 thermal watts. If the total fin surface of the copper coolant plates has an effective heat transfer coefficient of 2 Btu/hr-sq ft-°F, the average difference in temperature between the air and the metal is about 25°F because the total surface area of the fins is about 7 sq ft. This temperature rise is not excessive. If a permissible air-temperature increase of 10°F is allowed along the face of the stack, the required air flow is 42 ACF/min for a linear velocity of 40 ft/s. The estimated pressure drop across the stack, including inlet and outlet restrictions, is about 1.7 in. wc for a blower power requirement of 20 watts (if the blower is 50% efficient). Because of the high thermal conductivity of the copper plates, the actual temperature difference within the cell is about 7°F. Although the temperature rise within the cell is low — only double that estimated for the liquid-cooling plates — the blower power requirement is excessive. To reduce the blower power, we must reduce the air flow and consequently accept a higher temperature rise for the air as it passes through the stack. On the basis of a 25°F assumed temperature rise, the air velocity reduces to 16 ft/s and the total pressure drop decreases to 0.08 in. wc for a blower requirement of 3.8 watts. The blower power is now satisfactory, only about 4% of the electrical output of the three cell modules, but the temperature rise might be excessive within the stack. The two-dimensional heat transfer problem indicates that with the 25°F air-temperature rise, the temperature differential within the coolant plate would be about 18°F because the high thermal conductivity of the copper tends to stabilize the cell temperature. The

temperature difference across the cell could be further decreased by increasing the weight of the copper coolant plate. However, the 18°F is not excessive with phosphoric acid electrolyte due to the stability of the P_2O_5 . Because of the temperature differential, a concentration gradient will be imposed on the face of the cell. This concentration gradient is desirable so that the drier, incoming process air can first contact the colder section of the cell. As the process air also sets up a concentration gradient, these two gradients can partially cancel each other if the process air flows in an opposite direction to the cooling air.

5.7.3.2. Mechanical Construction

Two primary design features of the liquid coolant plate were used in the design of the air coolant plate — the Kel-F plastic insert for the gas manifold ports and the sweat-soldered copper construction. The problems in constructing the liquid coolant plate were avoided by improved design.

The primary components of the air coolant plate are illustrated in Figure 5.12, and an assembled plate is shown in Figure 5.13. The face plates for the air coolant plate were each generated by two layers of 0.010-in.-thick dead-soft copper sheet. Thus, four steel-on-steel embossings were required for each bipolar coolant plate. This procedure was simpler than the forming of the face plates for the liquid coolant plate, which used double this thickness. In that case, the work-hardening of the copper would not permit sufficient depth of embossing in one pressing, so reannealing and repressing were required. Satisfactory impressions were, however, obtained with a single pressing on the thinner stock.

The air passage waves between the face plates were generated by a deeply corrugated sheet of copper which extended the full length of the cell. This corrugated sheet was made by the Twinfold process in which each corrugation is made individually. The corrugations were 5/16 in. in overall height with adjacent grooves on 3/16-in. centers. Thus, the rounded sections of the corrugations fit into the valleys of the corrugated copper face plates on both sides of the bipolar coolant plates, assuring good electrical contact.

Reproduced from
best available copy.

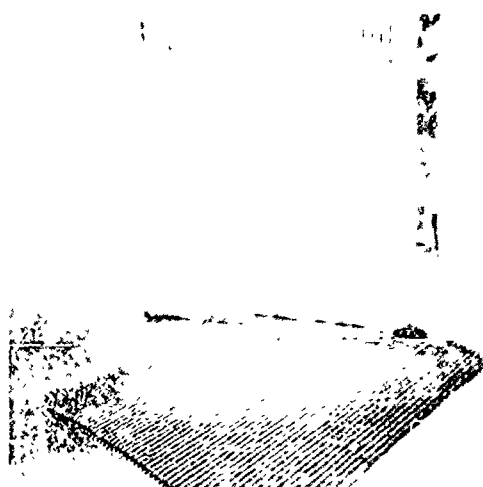


Figure 5.12. COMPONENTS OF AIR COOLANT PLATE

The gas manifolds were generated by Kel-F plugs, which were similar to those used on the liquid coolant plate but thicker to accommodate the increased depth of the air coolant plate. Grooves for O-rings were machined into the Kel-F plugs so that the gas manifolds could seal against the tantalum cover sheet for the coolant plate. The Kel-F inserts were retained by blocks machined from 1/4-in.-thick half-hard copper bar stock. The blocks for the gas outlet manifolds were located in the center of the coolant air inlet and outlet edges of the plate so the corrugated copper sheet, which extended to the edges of the plate, was cut away with 1/4-in. clearance around the block to permit gas flow in the center of the coolant plate. The four retainers for the gas inlet manifolds were located at the corners of the coolant plate. They were mounted in a jig, and the two retainers at each side of the coolant plate were interconnected by two lengths of 1/4-in.-square, half-hard copper bar stock by hard brazing. Again, the corrugated copper sheet

Reproduced from
best available copy.

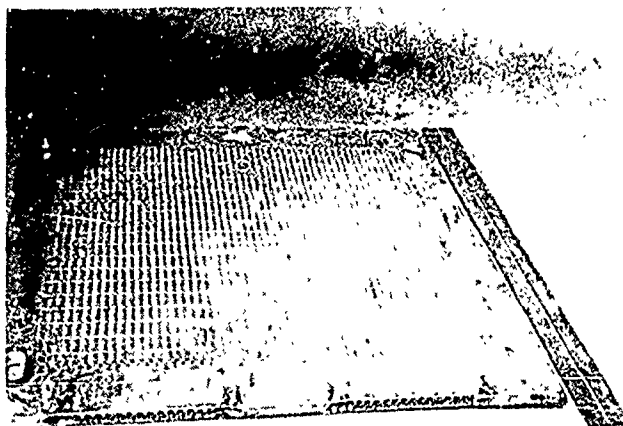


Figure 5.13. COMPLETED AIR COOLANT PLATE

was separated by 1/4 in. from the retainers to permit air flow in all of the corrugations.

All of the components were plated with 0.001 in. of tin — one-half the quantity used on the liquid coolant plates — and coated with a thinner layer of rosin. The tin foil was not used in assembly. The plates were then sweat-soldered to a solid unit by pressing for 2 hours at 550°F with a 10-ton force between the steel dies, which had been protected by prepressed stainless steel shimstock. The resulting plates were strong and less coated by excess tin solder.

The appearance of the plates was marred by two factors: The 5/16-in.-high Twinfold corrugations were unevenly crushed to 1/4 in. at the air inlets and outlets from the plate, and the copper face plate was slightly depressed and solder-filled in the region where the corrugated sheet had been clearanced from the bar stock manifold retainers. Neither

of these apparent defects caused operational difficulties on the first unit which was manufactured, and the handwork necessary to eliminate these problems was excessive. Therefore, the appearance defects were accepted.

The air-cooling plates were tested in a manner similar to that which had proved satisfactory with the liquid plates. The completed units were chilled with dry ice and exposed to high humidity until a layer of frost had formed. Then they were checked on the test station with the air blower. The rate of frost melting was observed and found to be relatively uniform, except it was slightly slower at the center rib and two end ribs, indicating a reduced air flow in these areas, perhaps due to insufficient clearance between the corrugated sheet and the copper manifold retainers. The differential melting rate was not high, however, so the design was accepted for the manufacture of the rest of the air coolant plates.

5.8. End Plates

5.8.1. Previous Design

The end plates of a fuel cell stack are the structural members which physically locate the cells and bind them together as a unit. In the IGT design, the end plates are larger in each dimension than the fuel cell unit, and the end plates are held together by bolts which interconnect them around the periphery of the cell stack.

The primary function of the end plates is as a compression device. They must transmit the forces of the bolts to the gaskets to ensure tight seals. A secondary function is flatness. The plates should have sufficient strength so that when the cell stack is compressed and the gaskets are sealed, the required forces do not cause significant bowing at the center of the end plate, as this would cause poor electrical contacts within the cell unit. A third function is to provide the outlets for the internal manifolding within the cell stack. These manifolds continue through the end plates with Kel-F inserts to avoid corrosion of the metallic end plates. The end plates are not under electrical potential because they are insulated from the cell stack by rubber gaskets.

The fourth function, which was used in the previous design, was to incorporate the coolant flow of the end modules within the end plates. The difficulties of flow restriction, pressure drop, and end plate bulging were discussed in Subsection 5.7.1. If an end plate had bulged, the deviation from the flat surface was compensated for by adding additional thickness of square hollow gaskets between the end plates and the first cell. However, the forces on the active area of the cell were not uniform with the end plates of the previous design.

The deflection of the end plate under load can be estimated by simple beam formulas. The total force on the older end plates, at a minimum, was sufficient to apply 100 psi loading on the 1-in.-wide peripheral compartment frame gaskets. Therefore, a minimum of 4400 lb was required; 50% greater forces were often necessary to effect a good seal of these gaskets. If the total force from the plate is 6000 lb and evenly divided among the peripheral bolts, the bolts on each side of the plate exert 1500 lb force. The counteracting force is the pressure on the gasket. If this is assumed to be exerted as a point at the center of the gasket, the maximum deflection of the stainless steel plate, if solid, would be 0.003 in. However, the plate is tied down on all four sides, an effect which reduces the deflection by about 33%, indicating a maximum deflection of the plate, if solid, of about 0.002 in. However, the plate had been hollowed for a coolant compartment so the effective moment of inertia was much lower, and the probable deflection was much greater than the 0.002 in. calculated.

5.8.2. End Plate - Structural Design

The end plates for the new cell were to be made of aluminum to minimize the weight of the stack prototype. Foundry castings were used; in production stacks, these castings might be made of magnesium to further reduce the stack weight.

Aluminum has only one-third the modulus of elasticity of steel, so the location of the forces and design of the end plate were modified to minimize the deflections.

The design of the gasketing within the new cell stack minimized the forces required upon the cell. The gasketing was a thin bead, only 0.031 in. in diameter. This would flatten during the stack compression to about 1/8 in. wide, so a force of only 25 lb per linear inch of the gasketing beads would be required to exert a sealing force of 150 psi. However, this low force is difficult to apply evenly to the end plates. The end plates were tied together by bolts. Springs were used between the other end plate and the free end of the bolt. These small die-springs had a rate of 400 lb/in., so only a 1/8-in. compression spring would apply 50 lb on each bolt. This corresponded to approximately 30-lb force per linear inch for gasketing.

The forces within the plate are a function of the distance between the bolts and the gasketing material. The gasketing bead is in the extreme edge of the compartment frame on the new design, compared with the average width of the compartment edge in the previous design. Similarly, the tie bolts were moved inward on the new design to minimize this distance. With the above considerations of loading and bolt-to-gasket distance, the deflection of a 1/2-in. plate of aluminum calculated as a simple beam is over 0.004 in. With the credit taken for loading around the periphery plate, the deflection is still excessive. The deflection would have been satisfactory with a plate thickness of approximately 3/4 in.

However, a lighter plate could be made by generating a structural bridge work above the flat bearing surface. Figure 5.14 is the engineering drawing of the structure which evolved, and Figure 5.15 is a photograph of the finished end plate. Calculations indicate that this end plate will have a maximum deflection of less than one-half of 1/1000 in. under load.

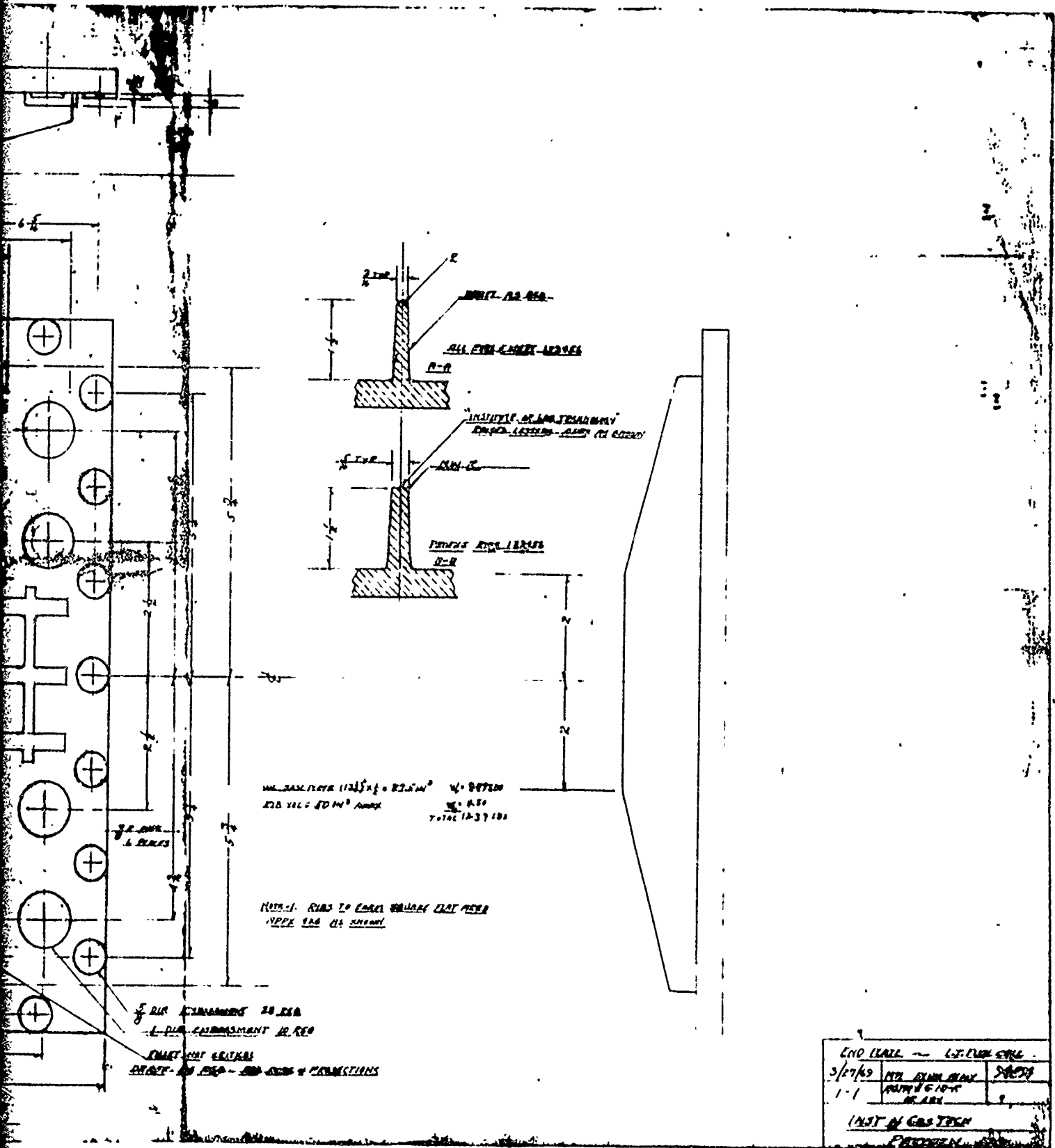
5.8.3. End Plate - Construction

The end plate was to be cast of aluminum by sand foundry practices to determine if this simple type of construction were possible. A wooden pattern of the end plate was made according to the design of Figure 5.14. Note that this pattern includes raised bosses for the bolt locations and for each of the 10 internal manifolds which were required under the philosophy of liquid coolant. This pattern was then used to make sand castings in Type A356 aluminum at the Research Foundry of Magcobar

[illegible]

71

B



PATTERN DRAWING OF END PLATE

A

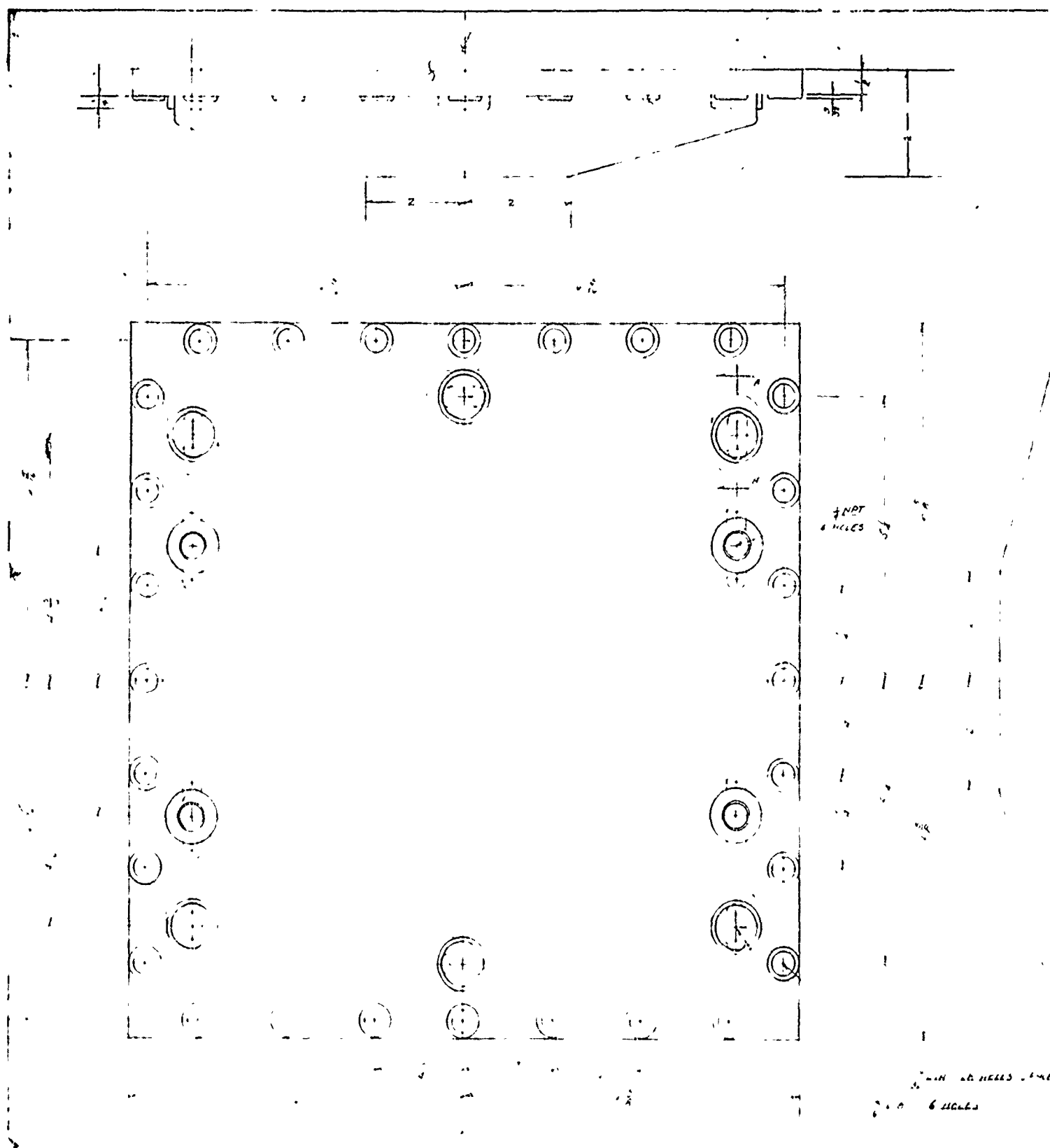
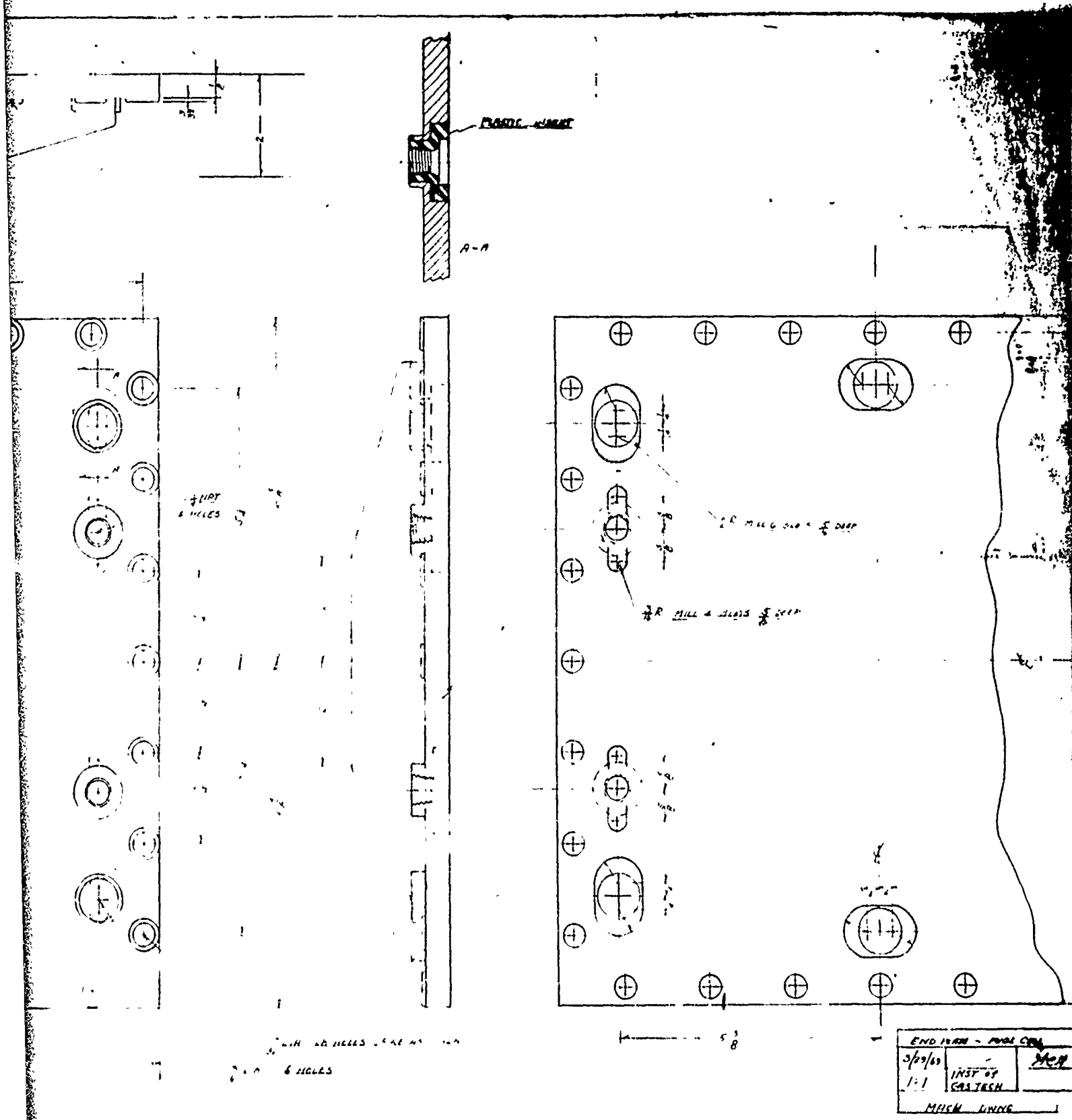


Figure 14b. MACHINING DRAWING OF END

B



END VIEW - FROM C		
3/29/53	INST BY	MEP
1:1	GRATISH	
MICH LINDS		

MACHINING DRAWING OF END PLATE

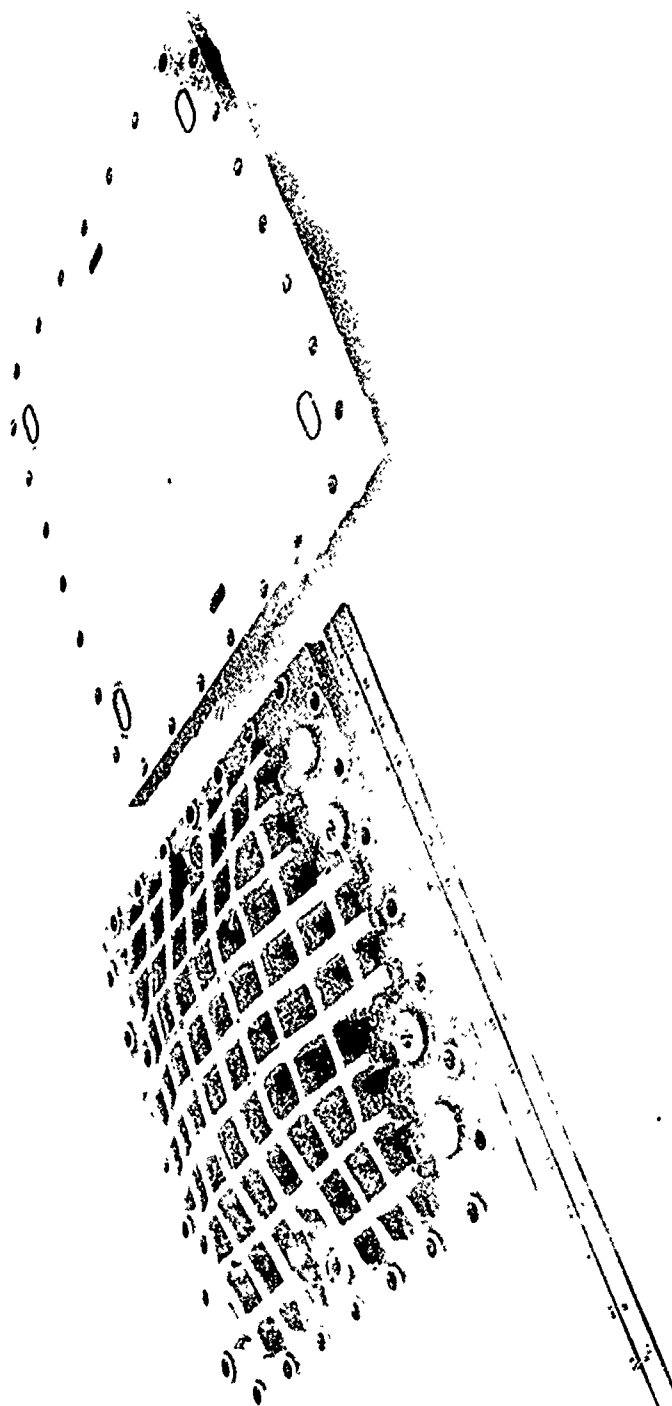


Figure 5.15. PHOTOGRAPH OF FINISHED END PLATES

Division of Dresser Industries. One reject casting was tested to 150-ton simple beam loading without failure, indicating the strength of this design.

The face of the end plate was machined flat, and the holes were drilled for the tie bolts. Cavities were also drilled for Kel-F inserts at each of the manifold locations. These inserts were oval-shaped, with a corresponding O-ring groove on the inside of the end plate to match the insert in the bipolar coolant plates. The external connections of these inserts were female pipe threads to connect with the gas or coolant external systems.

5.9. Assembly

The cell stack was assembled as modules. A module of three cells was built between cooling plates by placing each layer in position in order. First, the coolant plate assembly was laid down and 2-in.-long oval inserts were placed in the four inlet gas manifolds, forming a jig for the rest of the components. Then, an oxidant plate assembly was located on the jig. An oxidant plate consisted of a bipolar plate with oxidant-sized inlet orifices on one side of the plate only. This unit was an assembly because the plate, compartment frame, and gasket beading were sealed together as a unit during the gasket curing. Then an electrode was located, and a double, wetted matrix was located by means of the jigs. Then, the CO-tolerant anode was located. The next layer was a bipolar plate assembly which consisted of a bipolar plate with fuel inlet orifices on the bottom and air inlet orifices on the top, together with the associated compartment frames and gasket beading. The remaining cells were added in a similar sequence until three cells had been constructed, and the top plate was the fuel-only plate. Then, another coolant plate assembly, complete with gas manifold plugs and Viton O-rings, was located by means of the jig. The oval-shaped jig pieces were removed, and the module was ready for assembly between the end plates. If a three-cell module was being tested, the bottom end plate, with its gas outlet passages, was laid down, and a full-size rubber gasket, complete with bolt holes and gas outlet holes, was placed on the end plate. Then, a 0.016-in.-thick rubber gasket, 12 in. square with a 10-in. internal hole and gas manifold outlet holes, was located to compensate

for the distance between the top of the ridges in the face of the coolant plate and the load-bearing surface of the coolant plate. Then the module assembly was located, followed by similar rubber gaskets and the top end plate. Allen head bolts with nuts, washers, and calibrated die springs were used to tie the two end plates together. The force of the machine bolts was exerted against the die springs so that low loadings were obtained by measuring the compression of the die spring. Each of the 28 bolts was tightened evenly until all machine bolts had a tensile force of 50 lb as determined by a 1/8-in. compression of the springs. The assembly was then ready for testing. Figure 5.16 illustrates such an assembly of a single module using liquid coolant plate, and Figure 5.17 illustrates a 12-cell stack using the end plates.

Reproduced from
best available copy.

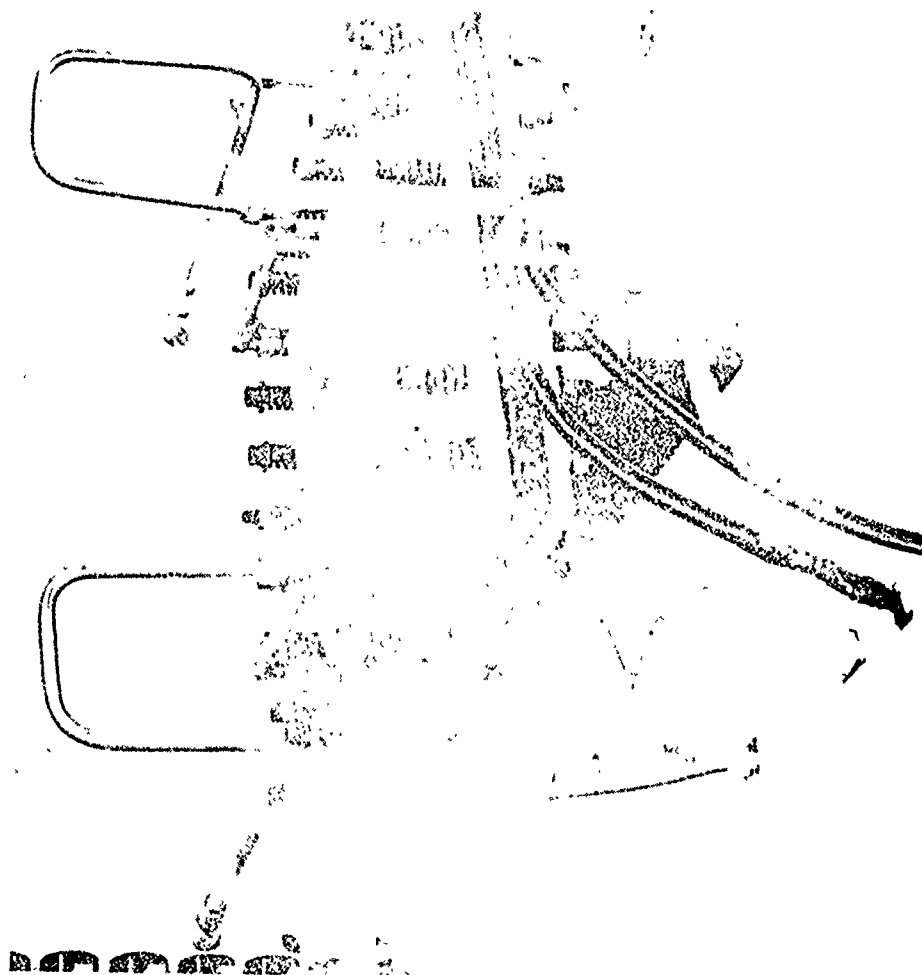


Figure 5.16. THREE-CELL MODULE
(Liquid Coolant) ON TEST

Reproduced from
best available copy.

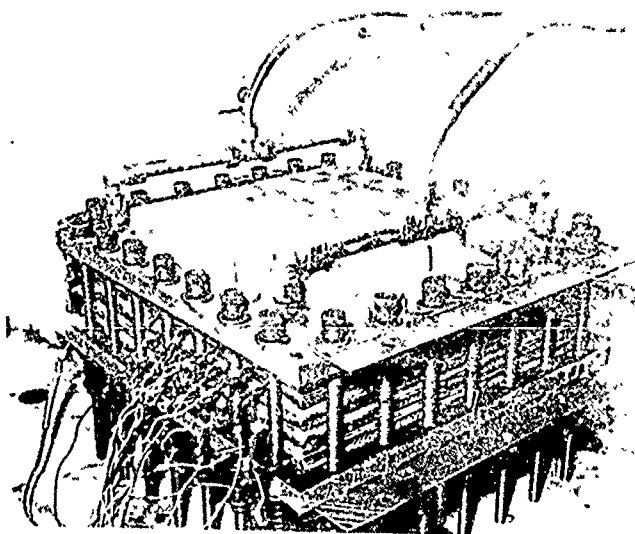


Figure 5.17. PHOTOGRAPH OF 12-CELL
STACK (Air-Cooled)

6. TESTING AND OPERATION

Several tests with smaller individual cells, smaller area stacks, and three-cell modules for the design stack were run before the actual operation of the nominal 100-sq-in. multicell stack. The discussion of these tests is presented below.

6.1. Small-Cell Tests

A series of tests were run on 4-sq-in. cells to test the performance of the individual electrodes received from the supplier. The purpose of these tests was to find 15 pairs of electrodes with uniformly high performance for use in the fuel cell stack.

The nominal area of an individual cell in the redesigned stack was 100 sq in. However, the length of the ribbed area was only 9-3/8 in. effective because of the radius of the curvature of the mill cutter. In other words, the ends of the grooves were not effective in forcing the electrode against the matrix. The inlet orifice design, in combination with the parabolic compartment frame, required a dead plenum at each end of the ribbed area. Therefore, slightly over 1/4 in. was lost at both the top and bottom of the ribbed area of a cell. The extra 5/8 in. x 10 in. of electrode material was used to select the superior electrodes from the lot which was purchased.

A single cell with 4 sq in. of active area was used to test the electrodes. The small 2 in. x 2 in. electrodes were made from the candidate sheets in four strips of 1/2 in. x 2 in. These electrodes were run with glass-fiber matrices containing 85% phosphoric acid in a single set of fuel cell hardware. The hardware consisted of tantalum end plates, drilled to provide effective gas distribution, with Teflon gaskets and spring-tantalum expanded metal for current collectors.

The hydrogen-oxygen and hydrogen-air performances of the electrodes at 200°F were used as a basis for selecting electrodes for the fuel cell stack. The anodes were uniformly active; the minimum of 15 anodes were tested to find enough anodes for the stack. The cathodes, however, were not so uniform. The maximum performance on hydrogen-air was 750 millivolts at 100 A/sq ft, IR-free. The arbitrary cutoff voltage was selected at 575 millivolts under the same conditions. Twenty-one cathodes

were tested to find 15 which exceeded this specification. We do not condemn the other electrodes; unknown factors in the small-cell testing might have had an influence. This testing was only a technique to prejudge and select the electrodes to be used, based upon a small strip from the edge of the electrode.

We note, however, that the variation in cell performance from test to test was greater than we had experienced in the past. This might be because of the testing of just the edges, which might be nonuniform, of the larger electrode, or to an intrinsic variability in this batch of electrodes.

6.2. Small-Stack Tests

A few tests were made with three-cell stacks of 0.25-sq-ft nominal electrode area to determine the optimum compartment frame thickness to correspond to the more deeply grooved plates and to evaluate candidate matrix materials.

The tests for determining the optimum compartment frame thickness were discussed in Subsection 5.3.2. These tests used existing hardware design, but with new bipolar plates. The new bipolar plates were made of columbium and pressed on a die that had been cut with the new wave-shaped cutter. Cross-grooves were not used. The stack was built with Teflon compartment frames of various thicknesses as indicated by the preliminary water-removal tests. Several tests with different configurations of gasket thicknesses were tried before the 0.025-in.-thick compartment frame was selected based upon minimum cell internal resistance, minimum pressure drop, and maximum cell output (indicative of blinded electrode area).

Tests of matrix material were made with the same hardware as the compartment frame thickness tests discussed in the preceding paragraph. These tests were presented in more detail in Subsection 5.6. At the time of these tests, only two high-temperature matrix materials were available — the American Cyanamid Teflon matrix and the Union Carbide tantalum oxide matrix. The cell outputs from both of these matrices were similar; the choice between the two matrix materials was made upon physical characteristics.

The Teflon matrix was dimensionally unstable. Significant shrinkage or stretching was experienced with this material in the preliminary tests, although that effect could be modified with sufficient impregnation of the matrix edge with Kel-F. Nevertheless, the dimensional instability was an awkward problem considering the relatively close tolerances of the cell stack in the areas of the gas manifolds. More disadvantageous, however, was the chemical instability of the Teflon matrix. When it had dried out, it would become hydrophobic and could not be re-wet. This was the primary factor that prevented its selection as the candidate matrix for the cell stack.

The Union Carbide tantalum oxide matrix material was extremely fragile. In particular, it would tend to crack along the line between the Kel-F edging and the untreated matrix material. This effect could be minimized by sanding the compartment frame corner smooth. Considering the deficiencies of the Teflon matrix material, the tantalum oxide was chosen for the cell stack.

The proprietary Pratt & Whitney matrix was not available at the time of the small-stack tests. When we decided upon its use at a later date, we based our decision upon its physical characteristics and not its electrochemical performance. We did not check its electrochemical performance because we were assured by Pratt & Whitney that it was satisfactory.

6.3. Large-Module Tests

The redesigned large-cell stack was composed of modules. Each of these modules was tested individually before the stack was assembled for operation. Individual cells, per se, were not tested electrochemically, but significant mechanical, pressure-drop, flow characteristics, inlet orifice configurations, and compartment frame thickness testing was done on dummy single cells of this size. These tests are discussed primarily in Subsections 5.3.2 and 5.3.3.

6.3.1. Liquid-Cooled Modules

Several attempts were made to build and test modules utilizing both internally and externally manifolded bipolar coolant plates. The modules were assembled according to the techniques outlined in Subsection 5.9, but satisfactory electrochemical testing was not accomplished because of the oil leakage problems that were discussed in Subsection 5.7.2.

6.3.2. Air-Cooled Modules

Each of the modules for the air-cooled fuel cell stack was separately built and tested before the entire stack was assembled. The modules were constructed according to the techniques outlined in Subsection 5.9.

Each of the modules operated satisfactorily, although not necessarily well. The operation of these modules is discussed in more detail in the next major subsection.

The purpose of the preliminary testing was to provide a means for preevaluation to permit substitution for defective components. However, because of the shortage of approved electrode and matrix materials, improvements of the pretested modules were not always possible. The critical shortage was that of sufficient matrix material. It was possible, with this testing procedure, to replace an end electrode without destroying any matrices. We could replace an interior electrode of either of the end two cells by destroying one matrix. However, we could not replace electrodes or matrix on the interior cell without destroying at least two matrices. This shortage of matrix materials precluded any component replacement on the internal cell.

6.4. Stack Operation

A 12-cell stack, designed as outlined in this report, was built and operated. This stack consisted of four modules of three cells each. The modules were separated by air-cooling plates and had been pretested before the stack operation. This subsection outlines the performance of that stack.

6.4.1. Design Criteria

The contract called for operation of a 350-W nominal output fuel cell stack with a 7-V terminal potential. Thus, a stack of this type would be one-quarter of a 1.4-kW, 28-V assembly.

A conservative design basis for reaching this power level was the operation at 50 A gross current through the 100-sq-in. nominal cell area (about 70 A/sq ft). Early in the program, we knew that 12 cells would be sufficient because of an average cell voltage of greater than 581 mV should be possible. To be conservative, however, the design was based upon a 15-cell stack (5 modules) with each cell operating at an average

of 465-mV potential. This conservative design basis allowed for significant possible poisoning of the electrodes, boot-strapping of a cold stack, or other contingencies which might require excess capacity.

The cell stack was to be operated with air for the oxidant and a fuel mixture simulating the product gas which would be obtainable from a single-stage low-temperature reforming of gasoline or CITE fuel. Such a mixture contains -

	<u>%</u>
Carbon Monoxide	2.4
Carbon Dioxide	22.3
Methane	11.0
Hydrogen	64.3

The electrodes chosen for this stack were the American Cyanamid Type AA-3 cathode containing 5 mg Pt/sq cm and the Type RA-2 anode containing 5 mg noble metal/sq cm. The anodes contain 50% platinum and 50% rhodium with tungsten oxide admix for maximum tolerance to carbon monoxide poisoning. The electrolyte for use in this stack was 85% phosphoric acid, and the temperature of operation was 250°-275°F.

The components of the cell stack had been redesigned for minimum pressure drop, maximum gas utilization, and for resistance to corrosion at the operating temperatures.

6.4.2. Design Compromises

Several compromises in the design of the stack became necessary during this program:

1. The program plan called for gold-plating the tantalum bipolar plates for minimum contact resistance. The initial cost estimated by the supplier for this plating was reasonable, but the final quoted price was prohibitive. The difference in performance attributable to the higher resistance of the bipolar plates was approximately 125 W on a 12-cell stack.
2. The maximum number of cells that could be operated in the stack was 12 because of a shortage of electrodes and matrices. The electrode supplier discontinued his program of commercial manufacture of fuel cell electrodes midway through this design program. Several electrodes were lost to oil contamination during preliminary testing with liquid-filled cooling plates, so that the maximum number of modules we could test was four. We had enough electrodes for 12 cells, but not 15. Even so, some of the electrodes used did not pass the preliminary screening discussed in Subsection 6.1.

3. A shortage of satisfactory matrix material developed. The most desirable matrix material tested in this program had been manufactured by Pratt & Whitney. However, its work had progressed to later generations of matrix structures that were not available for this program. Its stock of the older material was limited and too small for a single sheet to cover the entire cell. A method was developed for overlapping two smaller sheets of P&W matrix material, so that the remaining P&W inventory could be used. Each of the cells used a double matrix because even the stronger P&W matrix was not completely reliable in a single layer. Nevertheless, there was insufficient material to make double matrices of the P&W material for all 12 cells. Extensive use was made of the tantalum oxide as one layer in many of the cells. One cell used a double layer of the tantalum oxide matrix; this cell failed because of gas crossover, presumably due to a ruptured matrix.

6.4.3. Design Deficiencies

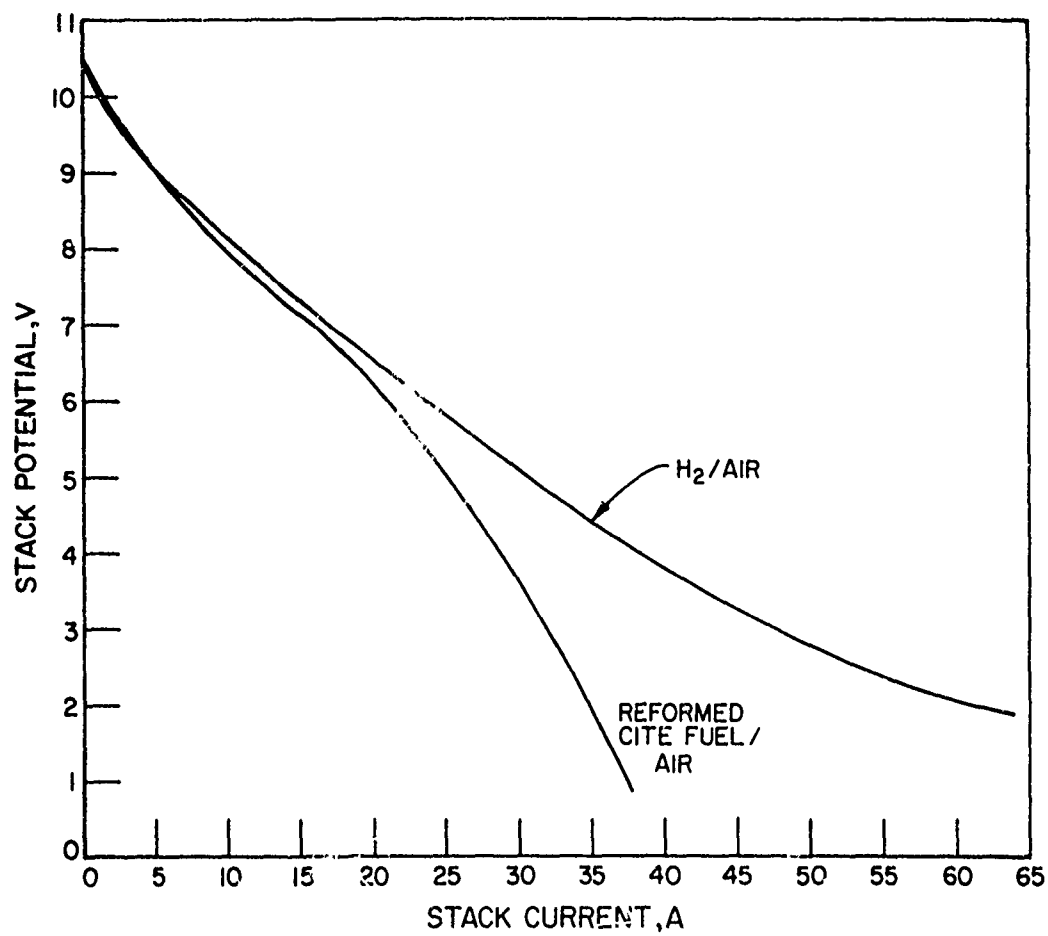
1. The primary design deficiency was the lack of consideration of the normal acid recharging required for this type of electrode material. In the previous program, we had found that a weepage of acid from the matrix occurs through the electrode, but that replenishment of the acid is required every 250-500 hours of operation. This stack design did not have a satisfactory method of adding that acid. Each of the modules had been previously tested, and when the stack was assembled, the assembly was resoaked with acid added through the gas inlet ports, similar to the technique that had been used in the earlier design. These were the only ports that could be used for acid recharging with the stack mounted on the test stand because of the configuration of the gas inlet and outlet ports in the end plate. As a result, some of the small gas inlet orifices became blocked with acid caused by the surface tension of the electrolyte. Similarly, there was no means for draining the gas inlet manifolds of excess acid, and the performance of the bottom two cells in the stack indicates that puddles of electrolyte remained in the bottoms of these manifolds. A more satisfactory acid recharging technique would have been addition of acid through the gas outlet manifold (and the larger gas outlet bridges) with draining through the gas inlet manifolds. This could be accomplished by adding suitable additional ports to the fuel stack end plates and insulating rubber gaskets.
2. The design of the gas outlet bridges was unsatisfactory. The performance of some of the cells during module testing indicated that some of these bridges might have been collapsing. A more satisfactory solution would be the use of small tantalum structural members, directly spot-welded to the bipolar plate, which directly support a heavier layer of flame-hardened tantalum sheet. This sheet could overlap the compartment frame, and the size of the slot in the compartment frame would govern the gas outlet passage. As the gas outlet is not the controlling resistance in the cell, this design should be satisfactory.

3. Other operating problems also occurred. The wettability and porosity of the new matrix material was significantly different from the old glass-fiber matrix. The techniques that had been satisfactory for impregnating the edges of that matrix with Kel-F solution did not result in a satisfactory edge seal in these matrices. Consequently, some acid wicked through the edge seal, particularly in the region of the liquid manifold ports in the bipolar plates, causing corrosion of the tin-plating on the copper coolant plates. Similarly, the electrolyte wetting of the matrices was nonuniform. The electrolyte for some cells did not appear to be uniformly wetted, causing a reduction in cell effective area and increase in the internal resistance of these cells.

Another operating problem was caused by culmination of the other factors. The high cell resistance, coupled with the inferior performance of some of the cells, prohibited the operation at the design current density. Therefore, the stack did not reach the design temperature, and poisoning of the anodes resulted.

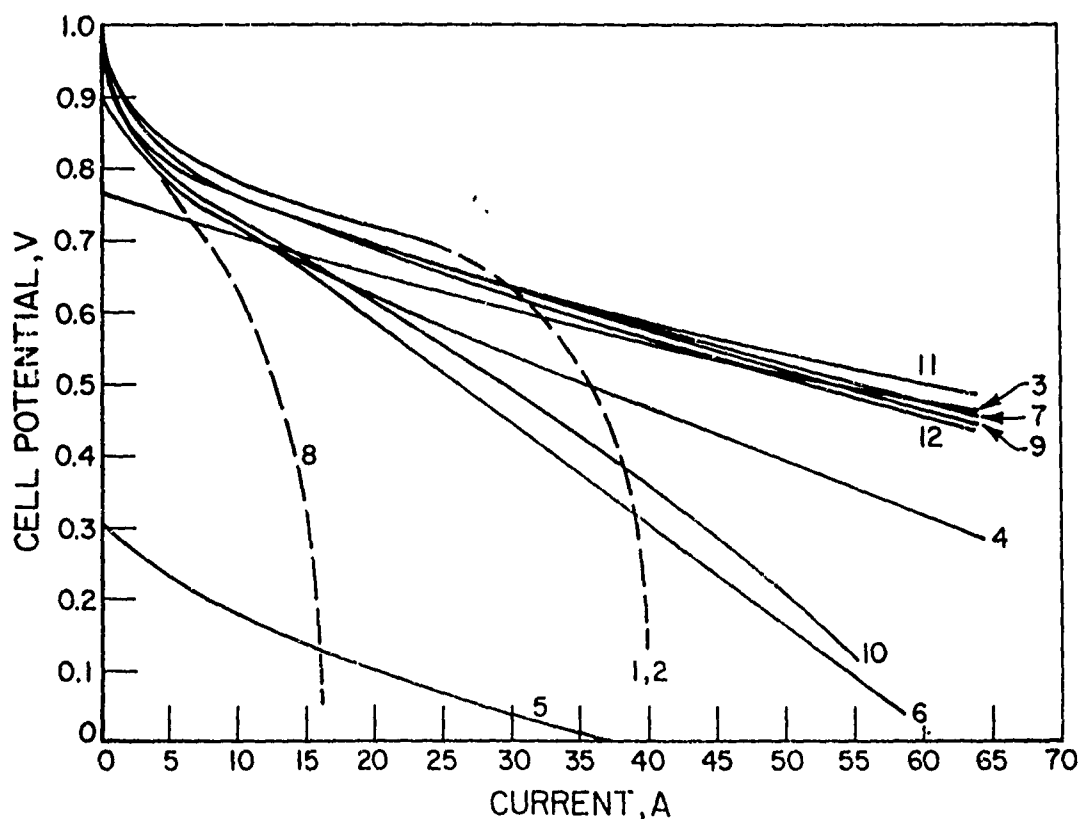
6.4.4. Operating Results

Figure 6.1 presents the operating performance of the fuel cell stack with air and both hydrogen and reformed CITE (2.4% carbon monoxide) fuels. Figures 6.2-6.4 present the performance of individual cells in this stack on hydrogen-air, hydrogen-air (IR-free), and reformed CITE fuel-air mixtures. Seven of the cells in the stack performed unsatisfactorily for various reasons, to be discussed below, but five cells yielded reasonable performance, considering the design compromises required. Figure 6.5 presents the performance of this stack if all cells operated according to the average of these five satisfactory cells. Note that the internal resistance of the stack is high, and poisoning of the anodes existed. Figure 6.6 presents the expected operating performance if the internal resistance of the stack were minimized and the operating temperature were high enough to minimize the anode poison. This graph indicates that the stack should have been capable of 437 W at the design potential of 7 V if all cells had been functioning and if the internal resistance were minimized. Thus it is apparent that the contract goals could have been met if time, electrodes, and matrices were available and if the gold-plating were done.



A-32264

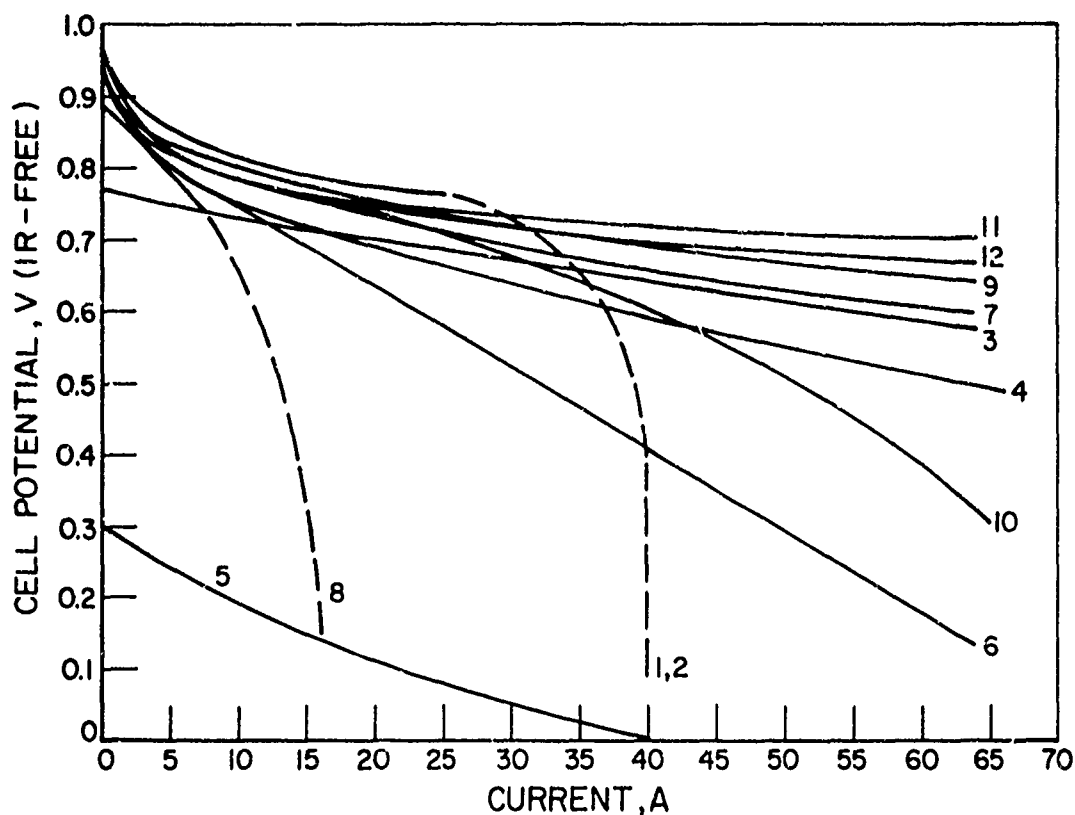
Figure 6.1. PERFORMANCE OF 12-CELL STACK



A-32262

Figure 6.2. PERFORMANCE OF INDIVIDUAL CELLS ON HYDROGEN-AIR

The above extrapolation is based upon the five cells which were operable to 100 A/sq ft. However, the IR-free potential of these cells varied by 120 mV at this current density. If the extrapolation is based upon the best of these five cells, the expected power output increases to over 600 W from a 12-cell battery operating at 7 V. A 15-cell stack, according to the original design, would have produced significantly more power because greater individual cell polarization could have been accepted at the 7-V output.

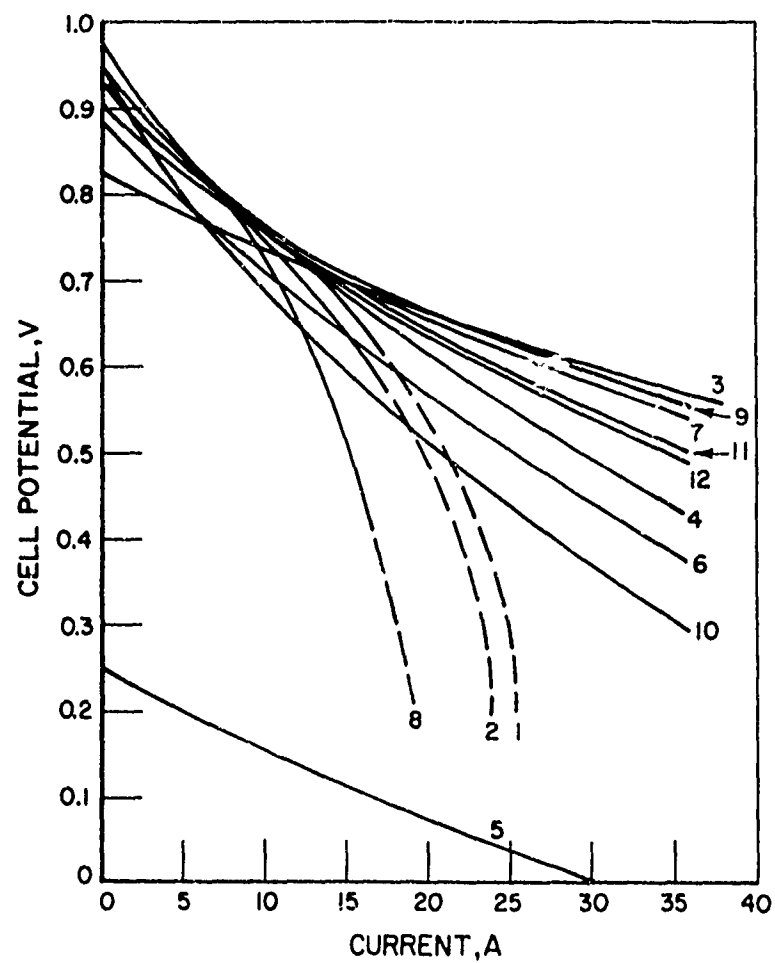


A-32263

Figure 6.3. PERFORMANCE OF INDIVIDUAL CELLS ON HYDROGEN-AIR (IR-Free)

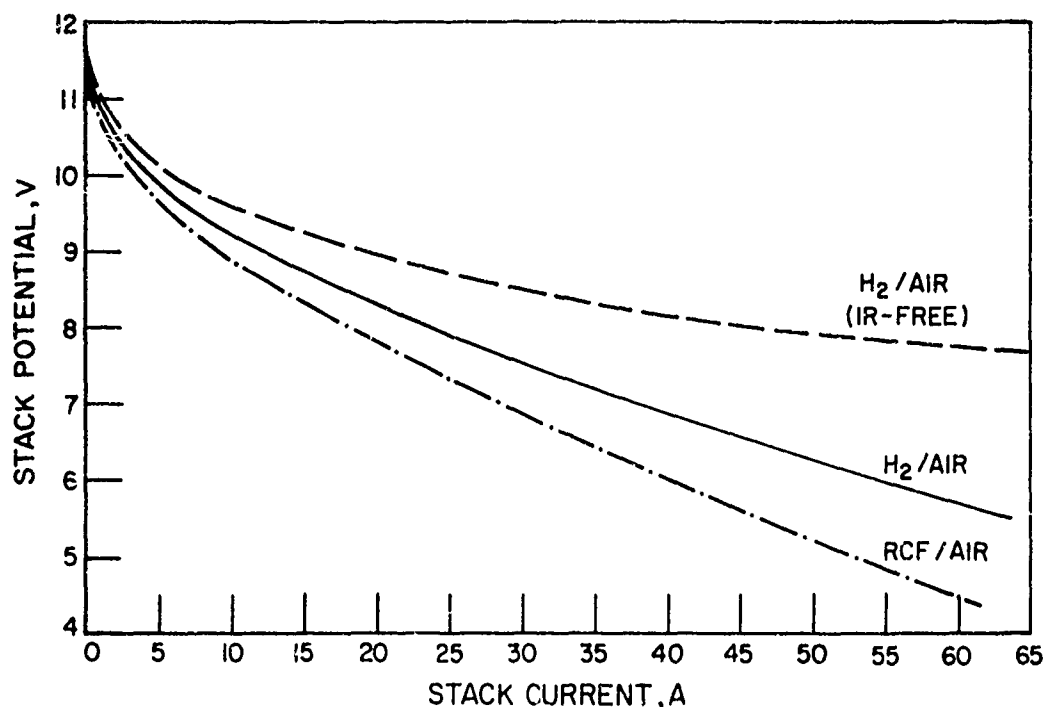
The performance of the individual cells in the operating stack is presented in Figures 6.2, 6.3, and 6.4. Figure 6.2 presents the gross performance on hydrogen and air of the individual cells while Figure 6.3 presents this performance on an IR-free basis. Figure 6.4 indicates the cell voltages when operating on reformed CITE fuel containing 2.4% carbon monoxide in the fuel.

Cells 1, 2, and 3 were in the bottom module of the stack. Cells 1 and 2 operated identically with oxidant starvation at 40 A gross current. Note that these cells would have been the best in the stack without the oxidant starvation. This starvation was probably caused by pools of electrolyte remaining in the inlet gas manifold after recharging the cells



A-32270

Figure 6.4. PERFORMANCE OF INDIVIDUAL CELLS
ON REFORMED CITE FUEL (2.4% CO) AND AIR

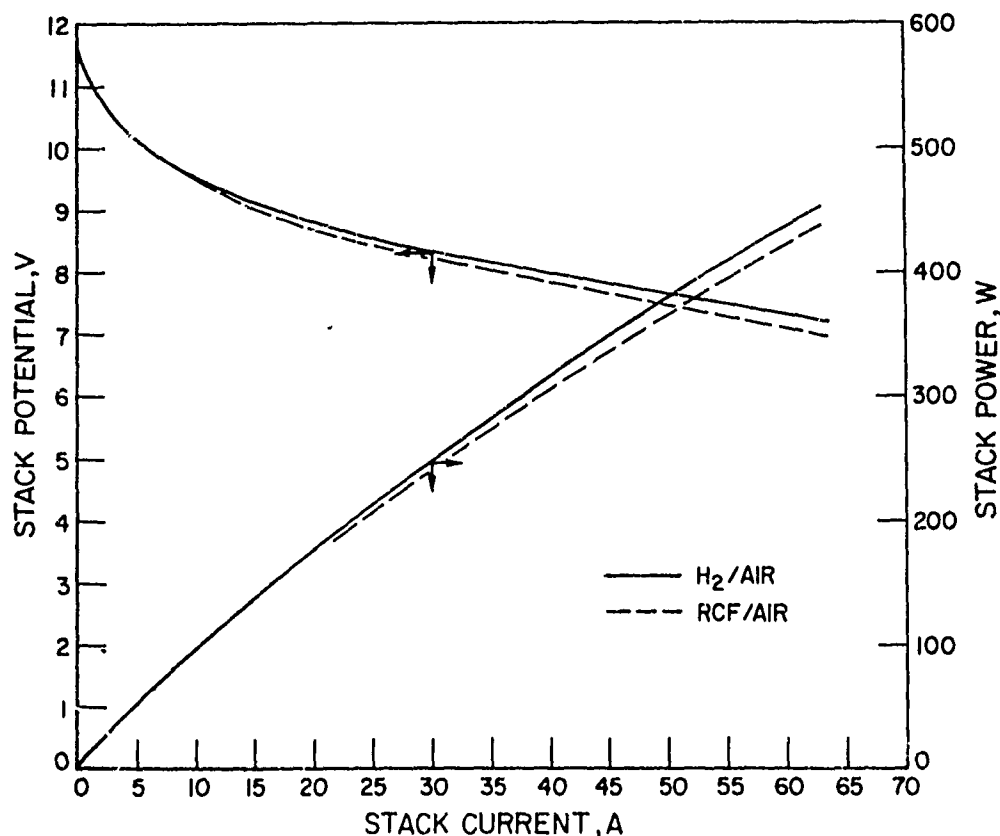


A-32265

Figure 6.5. EXPECTED PERFORMANCE OF 12-CELL STACK COMPOSED OF CELLS EQUAL TO AVERAGE OF FIVE BETTER CELLS

with electrolyte. Therefore, the oxidant for these cells had to enter those compartments through the normal exhaust port using oxygen-depleted air and using it ineffectively because of poor distribution over the face of the cell. Figure 6.4 indicates a similar effect of cells 1 and 2 for the fuel starvation; the performance on the dilute hydrogen is significantly poorer than with the purer hydrogen.

Cell 3 of this module apparently suffered from air crossover into the fuel compartment. The open-circuit voltage on hydrogen was only 770 mV, but this increased to 825 mV on the denser fuel. These effects indicate that a pressure imbalance existed in this cell, perhaps because of a restricted oxidant outlet, so that the oxidant was partially exhausted



A-32267

Figure 6.6. EXPECTED PERFORMANCE OF 12-CELL STACK WITH MINIMIZED RESISTANCE AT ELEVATED TEMPERATURE

through the fuel outlet. With the denser fuel mixture, the pressure in the anode compartment rose, forcing more of the air out of the oxidant outlet. After the initial module testing, it was noted that this cell had become dry. Perhaps it was not sufficiently rewetted during the electrolyte recharging operation.

The performance of the cells in module 1 would possibly have been the best in the stack without the operating problems discussed above. Certainly, cells 1 and 2 gave the highest performance at lower currents. This module was the first constructed and used double, full-sized P&W matrices throughout. It was the most extensively tested of the modules. The individual cell resistances were uniform at about 2 milliohms.

approximately triple that expected from the gold-plated hardware, and the electrodes were prescreened.

Cells 4, 5, and 6 constituted the last module to be built, perhaps explaining the uniformly poor performance. Cell 5 had only 302 mV open-circuit potential, but otherwise had reasonable polarization. Obviously, this cell had significant gas crossover, indicating a ruptured matrix. This cell used a double tantalum oxide matrix because of the shortage of the stronger P&W matrices. Evidently, this matrix failed.

Cells 4 and 6 used overlapping, narrow P&W matrices in combination with a single tantalum oxide matrix, and this combination was sufficiently strong that cell 4 had a reasonable open-circuit voltage of 930 mV, but cell 6 might have partially failed at an OCV of 895 mV. Neither of these initial performances, however, can account for the relatively poor performance of these two cells. All of the cells in this module used nonscreened electrodes, perhaps explaining the 100 to 200 mV deviations of cell 4 from the better cells. The poor performance of cell 6, however, cannot be so rationalized because it is below the range of the electrodes tested in the prescreening. Perhaps an oil-contaminated electrode, from the earlier liquid-cooling tests, was inadvertently used in this cell.

Cells 7, 8, and 9 comprised the third module in the stack. Cells 7 and 9 operated satisfactorily, but cell 8 suffered from oxidant starvation. The potential from this cell approached zero at only 16 A gross current, but improved as the oxidant pressure drop was increased. Apparently, both air-inlet orifices for this cell were plugged, perhaps by electrolyte, and it could only receive oxygen from the exhaust orifice.

Each of the cells in this module used a double matrix, one of which was a large P&W matrix. Cell 8 also used a large tantalum oxide matrix whereas cells 7 and 9 used overlapped smaller matrices for the reinforcement. None of these cells exhibited signs of broken matrices, but cell 8 had a high internal resistance indicative of nonuniform wetting of the matrix by electrolyte.

Cells 10, 11, and 12 were in the top module of the stack. Cells 11 and 12 operated satisfactorily; they were the best on an IR-free basis, but cell 10 exhibited operating problems. The internal resistance of cell 10 was approximately 6 milliohms, triple that of the better cells in the stack. This high resistance is probably caused in part by the non-uniformity of wetting of the matrix. Certain areas of the matrix appeared to have been blinded and would not accept electrolyte. On that basis, the effective area of cell 10 could be significantly less than the remaining cells in the stack. This was the third module to be assembled and matrices were in short supply, so an improperly built matrix was accepted. If the effective area of this cell were half of that of the other cells, its performance would be quite similar to the five normal cells in the stack. Additionally, this cell suffered slightly from air starvation; perhaps one of the air inlet orifices was partially plugged because the polarization increases at higher current.

Extensive use was made of overlapping P&W matrices in this module. Cell 10 had two pairs of overlapping matrices, while cells 11 and 12 used a single tantalum oxide matrix in combination with an overlapped matrix. No problems with gas crossover were noted in this module.

Figures 6.2 and 6.3 indicate that five of the cells operated similarly; the other seven showed decreased performance for the reasons mentioned above. Figure 6.4 illustrates the decreased performance of most of the cells when the fuel containing 2.4% carbon monoxide was substituted for the pure hydrogen. No significant concentration effects were observed, rather a general poisoning of most cells because of the effect of carbon monoxide at lower temperatures of operation. This effect would not have been severe at temperatures greater than 250°F, as evidenced by our earlier work under this contract number.

7. ACKNOWLEDGMENT

The talents of many people were necessary for this investigation. In particular, the effort and innovation of A. C. Allen, B. S. Baker, E. Camara, D. K. Fleming, D. Hegyi, and J. Valles are gratefully acknowledged as contributing significantly to the program.